

Review

Current international research into cellulosic fibres and composites

S. J. EICHHORN*

*Materials Science Centre, Grosvenor Street, UMIST/University of Manchester, Manchester, M1 7HS, UK
E-mail: stephen.j.eichhorn@umist.ac.uk*

C. A. BAILLIE, N. ZAFEIROPOULOS

Department of Materials, Imperial College of Science Technology and Medicine, Prince Consort Road, London SW7 2BP, UK

L. Y. MWAIKAMBO, M. P. ANSELL

Department of Engineering and Applied Science, University of Bath, Bath BA2 7AY, UK

A. DUFRESNE

Centre de Recherches sur les Macromolécules Végétales (CERMAV-CNRS), Université Joseph Fourier - BP 53, 38041 Grenoble Cedex 9, France

K. M. ENTWISTLE

Materials Science Centre, Grosvenor Street, UMIST/University of Manchester, Manchester, M1 7HS, UK

P. J. HERRERA-FRANCO, G. C. ESCAMILLA

Centro de Investigación Científica de Yucatán, A. C. Calle 43 # 130, Col. Chuburná de Hidalgo, C.P. 97200, Mérida, Yucatán, México

L. GROOM

USDA-Forest Service, Southern Research Station, 2500 Shreveport Highway, Pineville, LA 71360-2009, USA

M. HUGHES, C. HILL

School of Agricultural and Forest Sciences, University of Wales, Bangor, Gwynedd, UK

T. G. RIALS

USDA-Forest Service, Southern Research Station, 2500 Shreveport Highway, Pineville, LA 71360-2009, USA

P. M. WILD

Department of Mechanical Engineering, McLaughlin Hall, Queen's University, Kingston, Ontario, K7L 3N6, Canada

The following paper summarises a number of international research projects being undertaken to understand the mechanical properties of natural cellulose fibres and composite materials. In particular the use of novel techniques, such as Raman spectroscopy, synchrotron x-ray and half-fringe photoelastic methods of measuring the physical and micromechanical properties of cellulose fibres is reported. Current single fibre testing procedures are also reviewed with emphasis on the end-use in papermaking. The techniques involved in chemically modifying fibres to improve interfacial adhesion in composites are also reviewed, and the use of novel fibre sources such as bacterial and animal cellulose. It is found that there is overlap in current international research into this area, and that there are complementary approaches and therefore further combining of these may make further progress possible. In particular a need to measure locally the adhesion properties and deformation processes of fibres in composites, with different chemical treatments, ought to be a focus of future research. © 2001 Kluwer Academic Publishers

* Author to whom all correspondence should be addressed.

1. Introduction

Cellulose as a material is used by the natural world in the construction of plants and trees, and by man to make shipping sails, ropes and clothes to name but a few examples. Over the last few years a number of researchers have been involved in investigating the exploitation of cellulosic fibres as load bearing constituents in composite materials. The use of these materials in composites has increased over the last few years due to their relative cheapness compared to conventional materials such as glass and aramid fibres, their ability to recycle, and for the fact that they compete well in terms of strength per weight of material [1]. Natural fibres are classed according to their source; plants, animals or minerals. In general, it is the plant fibres that are used to reinforce plastics in the composite industry. Many varieties of plant fibres exist such as hairs (cotton, kapok), fibre-sheafs of dicotyledonous plants or vessel-sheafs of monocotyledonous plants (e.g. flax, hemp, jute and ramie), and hard fibres (sisal, henequen and coir), not to mention the large number of fibres obtained from trees. By far the most abundant are the wood fibres from trees (see Table I), however other fibre types are emergent in use. The abundance of the raw material is also a concern to the manufacturing industry, and the pressures on it to use evermore "greener" technologies has made this area of research of worldwide interest.

TABLE I Commercially important fibre sources [2]

Fibre source	Species	World production (10 ³ tonnes)	Origin
Wood	(>10,000 species)	1,750,000	Stem
Bamboo	(>1250 species)	10,000	Stem
Cotton lint	<i>Gossypium</i> sp.	18,450	Fruit
Jute	<i>Corchorus</i> sp.	2,300	Stem
Kenaf	<i>Hibiscus cannabinus</i>	970	Stem
Flax	<i>Linum usitatissimum</i>	830	Stem
Sisal	<i>Agave sisilana</i>	378	Leaf
Roselle	<i>Hibiscus sabdariffa</i>	250	Stem
Hemp	<i>Cannabis sativa</i>	214	Stem
Coir	<i>Cocos nucifera</i>	100	Fruit
Ramie	<i>Boehmeria nivea</i>	100	Stem
Abaca	<i>Musa textiles</i>	70	Leaf
Sunn hemp	<i>Crotolaria juncea</i>	70	Stem

Cellulose fibrils produced from animals have also gained importance as possible reinforcements in composite materials due to their high modulus, high aspect ratio and good compatibility with matrix materials.

Typical production values for commercially important fibre sources are summarised in Table I [2], and it is clear that only a change in market economics will promote the use of more plant fibre in favour of timber.

However, compared to conventional reinforcements such as glass and aramid fibres, problems exist with the variability of mechanical properties that one can obtain for natural cellulosic fibres such as flax and hemp. These, although fully exploited by the plant structurally, can cause anisotropy within the materials. In terms of strength and modulus, typical values are summarised in Table II [3] and one can see that the natural fibres compare quite well with glass (given their lower density), but are not as strong as both aramid and carbon.

The production of paper is an important process industrially, the understanding of which requires knowledge of the performance of fibres. In particular, the refining process, which breaks apart the fibres, has been studied quite extensively. The fact that focus has developed on reducing the amount of waste fibrous material in the process of papermaking has also led to the use of this excess material in the production of low-weight low-cost composite materials.

From a fundamental point of view, the deformation of cellulosic fibres is not well understood, this is due in part to inadequate testing regimes, and because local deformations within the fibres are particularly difficult to measure. When manufacturing composite materials, compatibility of the matrix and the fibres is also a problem, and various methods of increasing the adhesion between the matrix and the fibres have been investigated. These, and other problems that have been addressed recently, will be discussed in this paper.

2. Structure of cellulose

Before discussing recent advances in the measurement of the deformation of cellulose fibres it is apposite to discuss what is known about their structural components, which will be restricted to cellulose, hemicellulose, lignin, pectin and waxes.

TABLE II Mechanical properties of natural fibres compared to conventional composite reinforcing fibres [3]

Fibre	Density (g cm ⁻³)	Elongation at break (%)	Tensile strength (MPa)	Young's modulus (GPa)	References
Cotton	1.5–1.6	7.0–8.0	287–597	5.5–12.6	[4, 6, 7]
Jute	1.3	1.5–1.8	393–773	26.5	[4, 5, 6, 8]
Flax	1.5	2.7–3.2	345–1035	27.6	[6]
Hemp	—	1.6	690	—	[8]
Ramie	—	3.6–3.8	400–938	61.4–128	[6, 7]
Sisal	1.5	2.0–2.5	511–635	9.4–22.0	[4, 6, 8]
Coir	1.2	30.0	175	4.0–6.0	[4, 8]
Viscose (cord)	—	11.4	593	11.0	[7]
Soft wood Kraft	1.5	—	1000	40.0	[9]
E-glass	2.5	2.5	2000–3500	70.0	[10]
S-glass	2.5	2.8	4570	86.0	[4, 10]
Aramid (normal)	1.4	3.3–3.7	3000–3150	63.0–67.0	[10]
Carbon (standard)	1.4	1.4–1.8	4000	230.0–240.0	[10]

The term “cellulose” was first used by Anselme Payen in 1838 [11] when he discovered that when plant tissue, cotton linters, root tips, pit and ovules from the flowers of trees were purified with an acid-ammonia treatment, then followed by an extraction in water that a constant fibrous material was formed. Since then it has been generally accepted that cellulose is a linear polymer consisting of D-anhydroglucose units joined together by β -1,4-glycosidic linkages. The anhydroglucose units do not lie exactly in plane, but assume a chair conformation, with successive glucose residues rotated through an angle of 180° about the molecular axis.

Cellulose fibres can either be man-made (regenerated) or natural (native). The crystal structures of natural and regenerated celluloses are known as cellulose I and II respectively. In cellulose I the chains within the unit cell are in parallel conformation [12] and in anti-parallel conformation in cellulose II [13]. The other component of natural cellulose fibres is hemicellulose. This is not a form of cellulose but falls into a group of polysaccharides (with the exception of pectin) attached to the cellulose after the lignin has been removed. However, their structure contains many different sugar units, apposed to the D-anhydroglucose units in cellulose, and is a highly branched polymer compared to the linearity of cellulose. Lignin is a little understood hydrocarbon polymer with a highly complex structure consisting of aliphatic and aromatic constituents [14] and forms the matrix sheath around the fibres that holds the natural structure (e.g. trees) together. Pectins are a collective name for heteropolysaccharides, which consist of α -1, 4-linked galacturonic acid units, sugar units of various composition and their respective methyl esters [15]. Finally, the waxes consist of various alcohols and form a small percentage of the structure.

Cellulose is found not to be uniformly crystalline. However, the ordered regions are extensively distributed throughout the material, and these regions are called crystallites. The threadlike entity, which arises from the linear association of these components, is called the microfibril; it forms the basic structural unit of the plant cell wall. These microfibrils are found to be 10–30 nm wide, less than this in width, indefinitely long containing 2–30,000 cellulose molecules in cross-section. Their structure consists of a predominantly crystalline cellulose core. This is covered with a sheath of paracrystalline polyglucosan material surrounded by hemicelluloses [16]. In most natural fibres these microfibrils orient themselves at an angle to the fibre axis called the “microfibril angle” and it is to the measurement of this angle that we shall now turn.

3. UMIST—microfibril angle measurements

Ken Entwistle at the Materials Science Centre, University of Manchester has been using small angle and Wide Angle X-ray Scattering (WAXS) to measure the microfibril angle of sections of *Pinus radiata*. Wood fibres are composite sheath of several layers; the primary, S_1 , S_2 , and S_3 , of which the S_2 is the thickest and gives rise to the stiffness of the fibre [17]. The measurement of the microfibril angle of the cellulose in the S_2 layers

of the cell walls of softwood is an essential step in the process of understanding the elastic, creep and strength properties of a particular wood specimen.

A widely used technique for the measurement of the micro-fibril was developed by Cave [18]. Specimens with their cell axes vertical are irradiated in a direction perpendicular to one set of cell walls and the (002) diffractions from the cellulose fibres are recorded. It is not easy to extract a value for the micro fibril angle from the diffraction pattern because the diffractions from the individual fibres overlap. Cave has proposed a method of dealing with this problem, which involves drawing tangents to the extreme edges of the total intensity distribution round the (002) diffraction circle.

Ken Entwistle has developed an alternative method [19] in which the specimen is irradiated in a direction at 45° to both sets of cell walls. This shows that, in principle, all the fibres in the S_2 layers give rise to eight intensity peaks round the diffraction circle.

If we imagine a cell wall with its axis vertical and its normal at an angle α to the X-ray beam (Fig. 1a). Lying in the cell wall is a single cellulose fibril f with its axis at an angle M , the micro-fibril angle, to the vertical. The normal to the plane that satisfies the Bragg condition is p and r is the Bragg reflection. This produces a diffraction spot S on the detector plane and its azimuth angle ϕ is given by

$$\cot M = \frac{1}{\sin \phi} \{ \tan \theta \sin \alpha + \cos \phi \cos \alpha \} \quad (1)$$

where θ is the Bragg angle.

There is a second diffraction on the opposite side of the (002) diffraction circle at an azimuth angle ϕ^\perp given by

$$\cot M = \frac{1}{\sin \phi^\perp} \{ \cos \phi^\perp \cos \alpha - \tan \theta \sin \alpha \} \quad (2)$$

These two diffraction spots are not diametrically opposite. Fig. 2b shows a diffraction pattern from a set of parallel cellulose fibres from the common nettle oriented with $M = 45^\circ$ and $\alpha = 45^\circ$ which confirms this fact. The observed azimuth angles of 41.5° and 29° degrees are close to the values predicted by Equations 1 and 2.

Fig. 2a shows the irradiation geometry for a cell with four sets of fibres a, b, c and d and Fig. 2b shows the location of the eight diffraction spots for $M = 45^\circ$ and $\alpha = 45^\circ$. A plot of the intensity distribution round the (002) diffraction circle for a wood specimen irradiated under these conditions is possible. The two pairs of taller peaks are from the S_2 layers. The two lower peaks are from the S_1 and S_3 layers in which the cellulose fibres are almost horizontal. The expected eight peaks are not all resolved. Each of the four S_2 peaks is a composite of two adjacent peaks. The centre of each of these will lie at the mean angle of the two peaks, for example from fibres a and d or from b and c in Fig. 2b. The average azimuth angle for each of these peak pairs can be shown, from Equations 1 and 2 to be

$$\phi_{av} = \arctan(\cos \alpha \tan M). \quad (3)$$

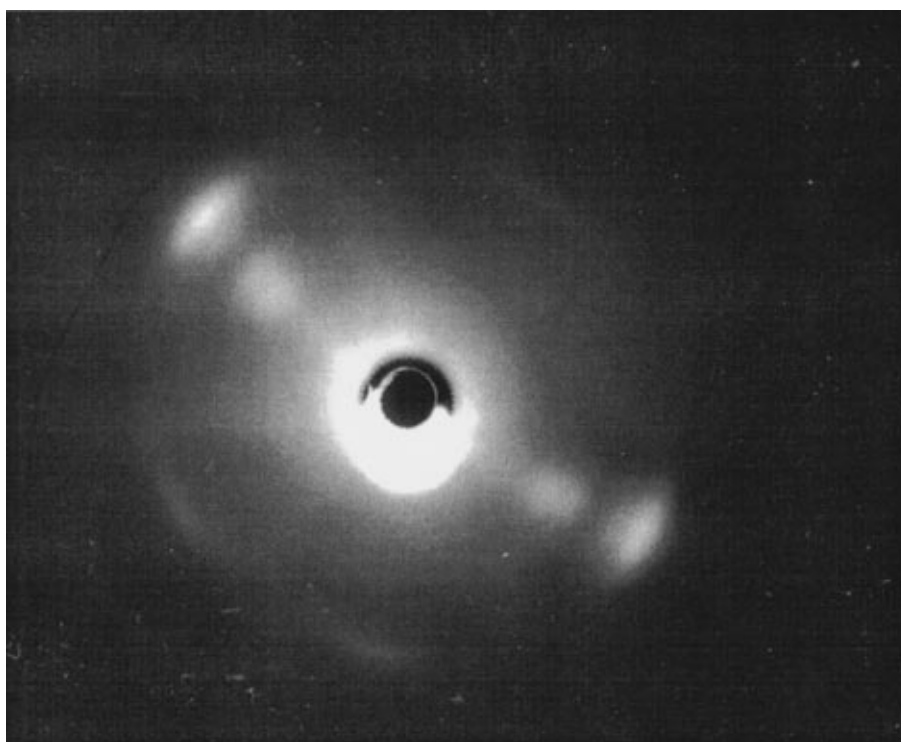
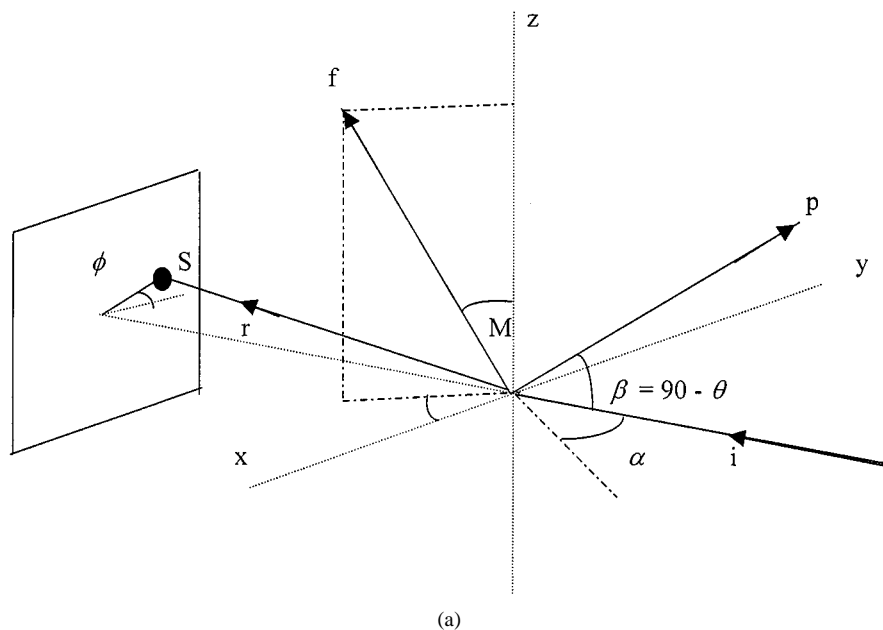


Figure 1 (a) Diffraction from a single cellulose fibre. (b) Wide angle diffraction pattern from a set of parallel cellulose fibres with $M = 45^\circ$ and $\alpha = 45^\circ$.

ϕ_{av} is found to be 21.7 degrees from an azimuthal scan, so the micro-fibril angle is

$$M = \arctan\left(\frac{\tan \phi}{\cos \alpha}\right) = 29.4 \text{ degrees.} \quad (4)$$

The cellulose fibrils have a diameter of about 25 nm. They are very much longer than this so the small angle scattering is confined to the direction perpendicular to the fibre axis. Using this fact it is possible to predict the orientation of the scattering streak in the detector plane for any orientation of the fibre in the X-ray beam. Fig. 3a is a diagram showing a fibril f in a cell wall

whose normal makes an angle α to the incident X-ray beam which is normal to the detector plane. The fibril lies at an angle M to the vertical. The scattering will be confined to the plane of the fibre cross-section. So the orientation of the scattering streak in the detector plane will be the line of intersection of the plane of the fibre cross-section with the detector plane. This is the line S in Fig. 3a. The azimuth angle ϕ of S can be shown to be given by

$$\tan \phi = \cos \alpha \tan M. \quad (5)$$

It is interesting to note that this is identical to Equation 3. If a specimen with the cell axes vertical is

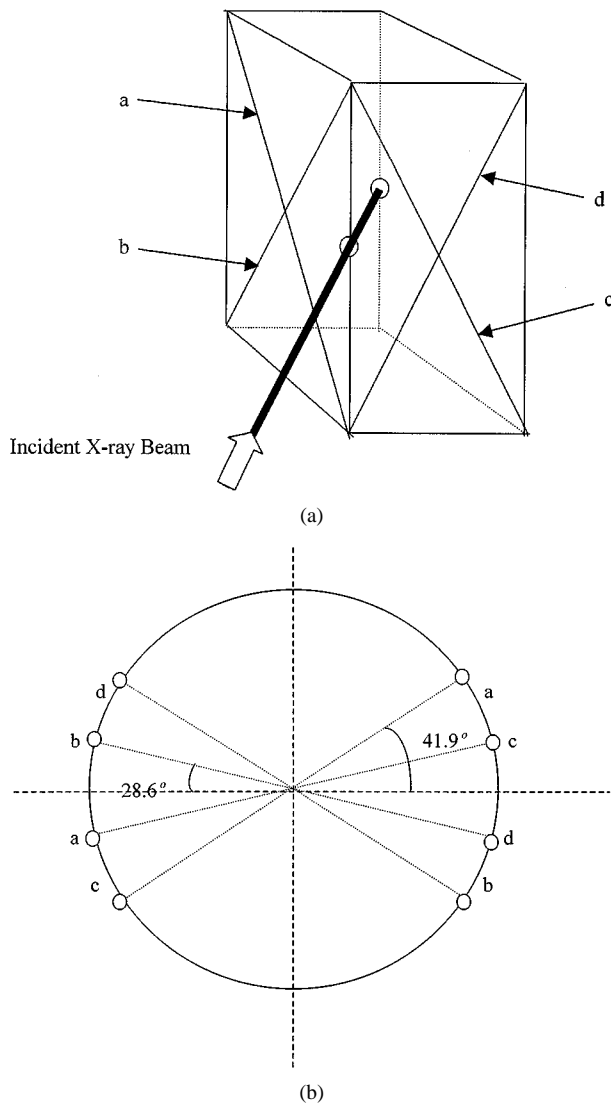


Figure 2 (a) Diagram showing the four sets of cellulose microfibrils, labelled a to d, in the two sets of cell walls. The x-ray beam is directed at 45° to both sets of walls. (b) Location of the (002) diffraction spots for the four sets of cellulose fibres when the X-ray beam is equally inclined to both sets of cell walls and the cell axes are vertical.

irradiated with the X-ray beam directed perpendicular to one set of cell walls, the set of small angle scattering streaks from all the S_2 fibres is shown in Fig. 3b. The streaks from the fibres in the front walls will lie at an angle $2M$ to each other, but the side walls, which are parallel to the beam, will produce strong streaks in the horizontal plane S_{sw} , which will obscure the front wall streaks. Fig. 3c is a small angle scattering pattern generated at the Daresbury Synchrotron which confirms this prediction. If alternatively the X-rays are directed at 45° to both sets of cell walls, as in Fig. 2a, streaks from fibres a and c and from b and d superimpose and a cruciform pattern is produced illustrated in Fig. 4a. The angle 2ϕ between the streaks yields a value for the micro-fibril angle M through Equation 4. Fig. 4b is a small angle scattering pattern that confirms this expectation. The measured azimuth angle ϕ is 20.6° so

$$M = A \tan \left(\frac{\tan 20.6}{\cos 45} \right) = 28^\circ \quad (6)$$

4. Micromechanical deformation

The need to adequately create an interface between the fibres and matrix material requires that the interfacial shear stress (a measure of the forces acting between the fibres and matrix) be measured. This is a particularly difficult measurement to make, and traditional methods of measurement of fibre pull-out, push-in and fragmentation give no information about the local stresses and strains in the fibre that can cause failure. This means that local stress and strain must be measured in the fibre and the following section deals with this problem.

4.1. UMIST—Raman deformation studies

Another group (Robert Young and Steve Eichhorn) at the Materials Science Centre, UMIST has been looking at using Raman spectroscopy to probe the micromechanics of regenerated and natural cellulose fibres. This technique relies on an effect discovered by Mitra *et al.* [20], and later theoretically explained by Batchelder *et al.* [21] wherein a characteristic Raman peak shifts towards a lower wavenumber upon the application of stress/strain. The technique has been applied previously to a large number of polymeric materials [22] and lately to cellulosic fibres [23–25].

The mechanical properties of natural and regenerated cellulosic fibres have been found to be completely different, with the natural fibres exhibiting near linear behaviour whereas the regenerated fibres show non-linear behaviour (Fig. 5). Coherent Raman spectra have been obtained in the region containing the 1095 cm^{-1} peak, which corresponds to the ring stretching modes of the cellulose structure [26]. This peak is found to shift upon straining to a lower wavenumber, which is thought to be due to the direct stressing/straining of the molecular backbone of the cellulose fibre. The shift rate with respect to strain has been found to be proportional to the modulus of the fibre (refer to Fig. 6) and invariant with respect to stress ($\sim 4.6 \text{ cm}^{-1}/\text{GPa}$) (refer to Fig. 7). This stress-invariance has led to the conclusion that the materials structure can be modelled using a modified series aggregate model structure [27, 28], as pictorially described in Fig. 8. In such a structure the stress is uniform and equal within each element (composed of crystalline and amorphous regions). The surprising result is however, that despite the different crystal structures of natural and regenerated cellulose (cellulose I and II) the rate of shift with respect to stress is equal for each type. The technique has proven useful for other cellulosic structures such as paper and wood and will be applied in the future for monitoring stress and strain within composite materials.

5. Single fibre testing procedures for papermaking

Papermaking fibres, traditionally from wood, behave differently at elevated temperatures and humidity, which are typically achieved during processing. Most research on the tensile behaviour of single fibres has been done at room temperature and humidity, and therefore for any meaning in terms of performance in the

papermaking process is lost. Also inadequate testing regimes for small fibres have given erroneous results. For example the size of the fibres being tensile tested means that specialised equipment must be developed in order to accurately measure stress and strain. Typical wood-pulp fibres for instance are usually about 1–3 μm in length, and therefore most of them are too small to be tested using conventional methods of gluing to fibre cards.

The following section reports some research done to overcome these problems.

5.1. Queens University, Kingston, Ontario—fatigue testing of single fibres
Peter Wild, Department of Mechanical Engineering, Queens University, Kingston, Ontario has developed such a testing device for conducting cyclic, axial and transverse loading of single wood-pulp fibres. In the past forty years, there have been many experimental studies of the effects of various types of loading on single wood-pulp fibres. Most of these studies deal with axial loading and most notable among these are the various works of Page [29–34]. Page’s work is, however,

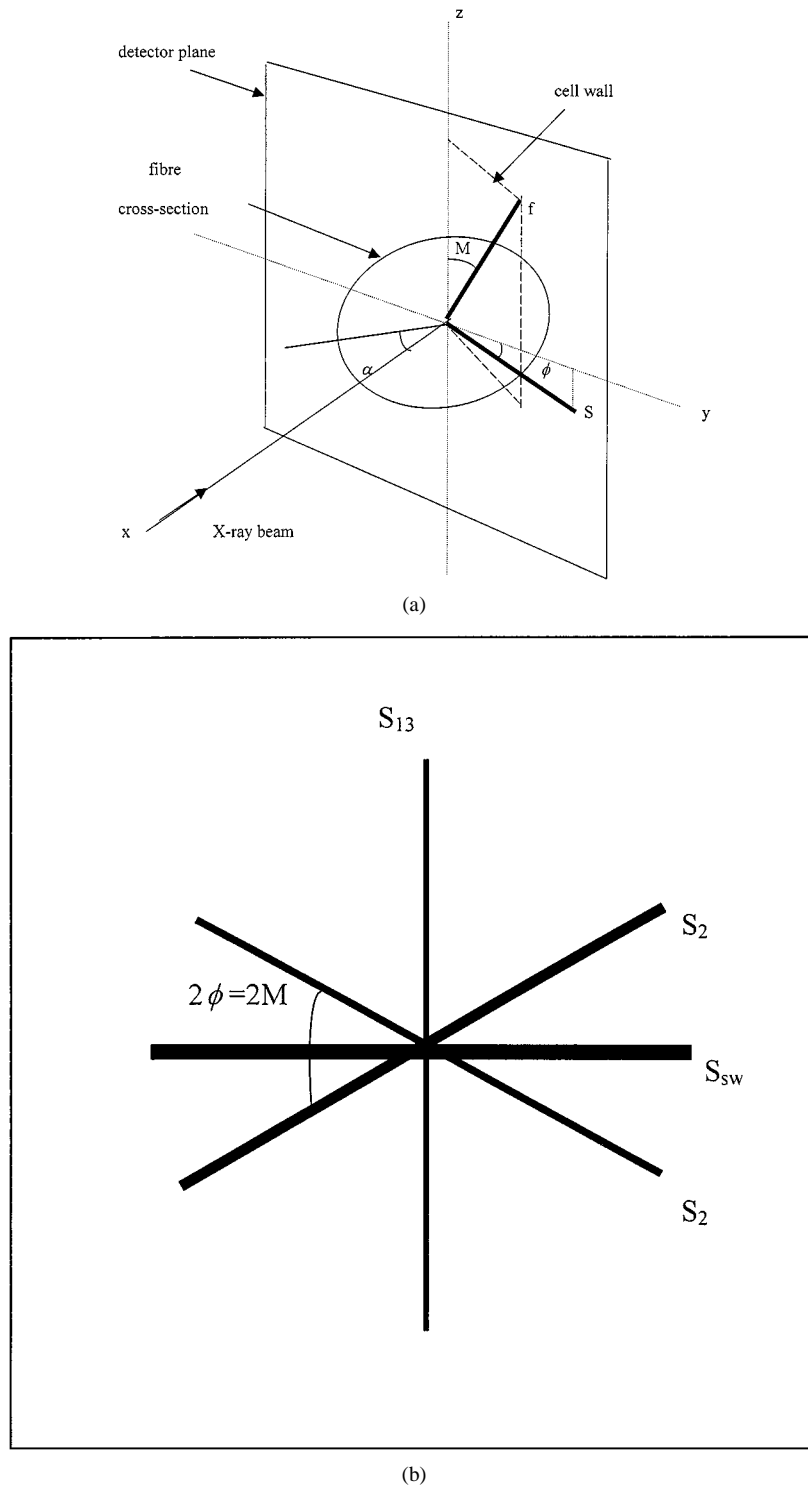
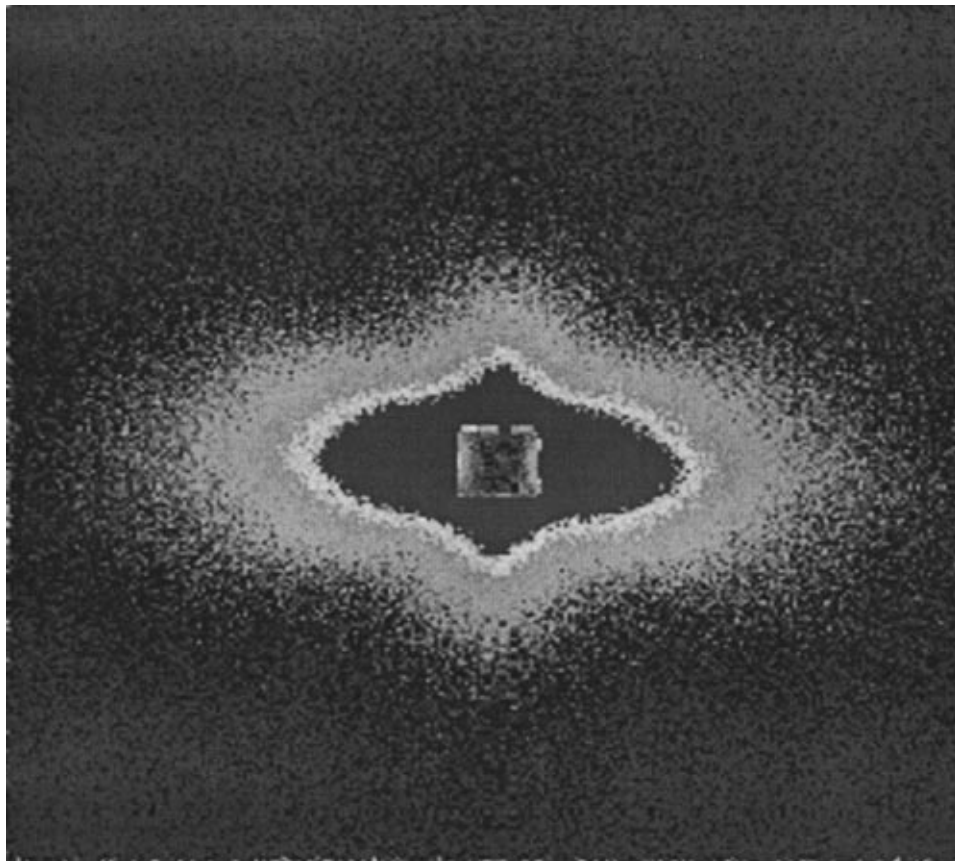


Figure 3 (a) Diagram showing the orientation of the SAXS streak S from a single fibre of arbitrary orientation relative to the X-ray beam. (b) Orientation of all the SAXS streaks from all the cell wall layers in wood cells irradiated with the X-ray beam normal to one set of cell walls. (c) Small angle scattering pattern from a *Pinus radiata* specimen with the x-ray beam directed normal to one set of cell walls. (Continued.)



(c)

Figure 3 (Continued).

limited to the effects of single load cycles. Kallmes and Perez [35] and Jentzen [36] conducted studies in which fibres were subjected to cyclic axial loading but the numbers of cycles were restricted to only six and three respectively, and at room temperature and humidity. Investigations of the effects of transverse loading are much more limited. Nyren [37] and Hartler and Nyren [38] are the only published works in this area. Again, these studies are limited to single load cycles and ambient temperatures and humidities.

The focus of Peter Wild's research has been the development of an instrument for the application of cyclic axial and transverse loading to single wood-pulp fibres at elevated temperature and humidity. The application of this instrument is to a variety of studies related to the development of an understanding of mechanical refining at the level of the individual fibre. Refining is the process whereby pulp fibres are processed, before papermaking commences.

The design and initial experimental results for the first generation of this instrument are reported in Wild and Provan [39]. The second generation of this instrument, shown in Fig. 9, can apply cyclic loads at up to 1 kHz while monitoring both the force applied to the fibre (0.1 mN resolution) and the elongation or compression (1 μm resolution) experienced as a result. The fibre is gripped using the epoxy droplet method, developed by Kersavage [40] and improved by Mott, Shaler, Groom and Liang [41]. Loads and displacements are applied using a levered piezo actuator. Forces and displacements are measured using piezo force transducers

and LVDT's, respectively. The fibre is located within an environmental chamber, which can be maintained at 100°C and 100% relative humidity.* The operation of the instrument is controlled using a PC based interface developed using the National Instruments software LabVIEW™.

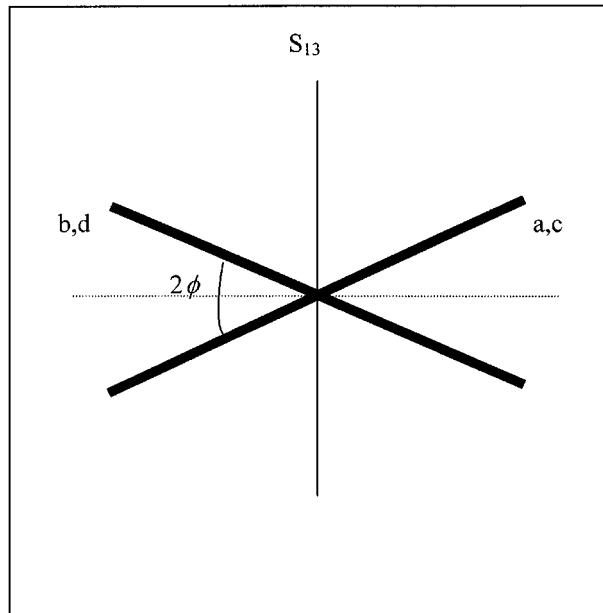
For cyclic axial tension, typical test data is as shown in Fig. 10 [39]. The first load cycle generates a linear force-displacement relation. Subsequent load cycles show successive but diminishing increases in the stiffness of the fibre as well as hysteresis associated with visco-elastic and plastic deformation.

For cyclic transverse compression, typical test data is as shown in Fig. 11. Note that the horizontal axis is fibre thickness. The first load cycle is characterized by two distinct regions in the force versus thickness (or displacement) plot. In the first region, corresponding to collapse of the lumen, the fibre has a relatively low stiffness. In the second region, corresponding to compression of the cell wall, the fibre has a relatively high stiffness.

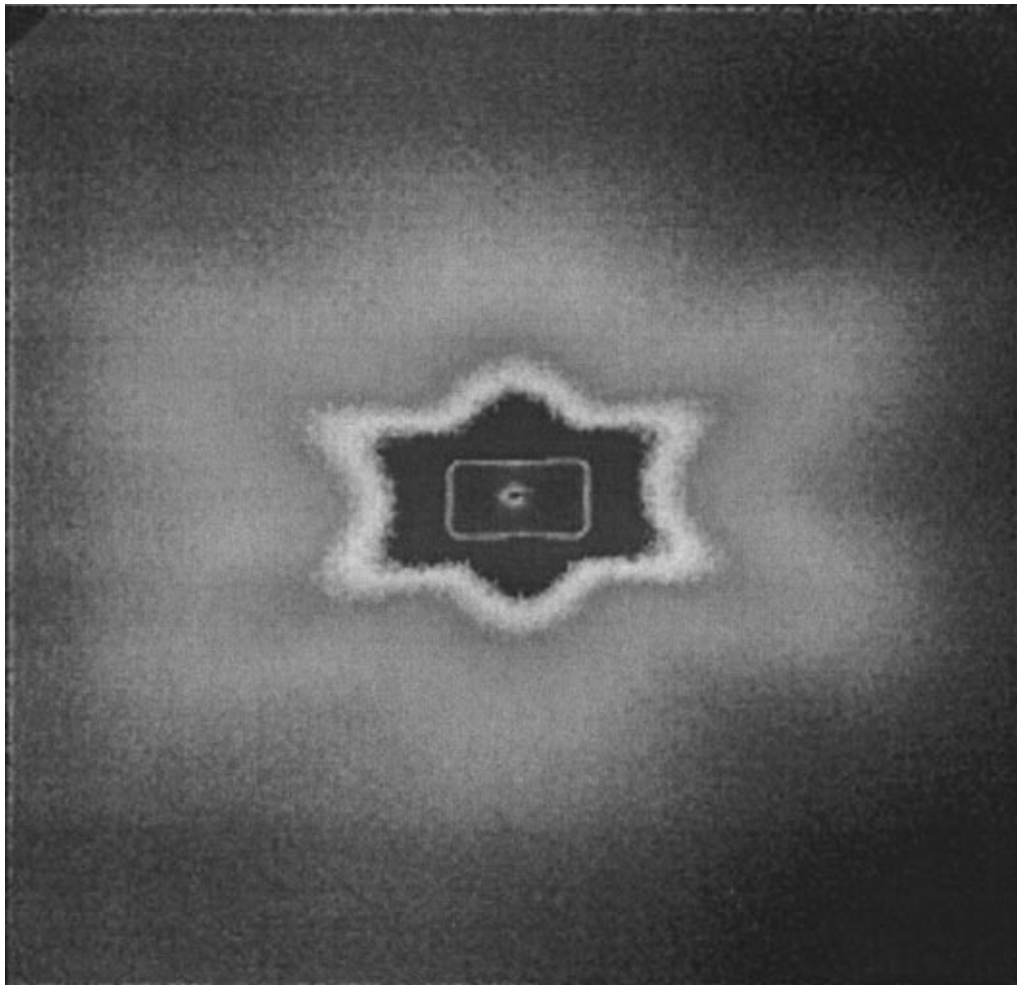
As in the case of cyclic axial loading, subsequent load cycles show successive but diminishing increases in the stiffness of the fibre as well as hysteresis associated with visco-elastic and plastic deformation.

This instrument presents the opportunity for a variety of studies of single fibre behaviour. Parameters to be investigated include: cycle frequency, stress amplitude, strain amplitude, temperature, humidity, species,

* Typical refining conditions.



(a)



(b)

Figure 4 (a) Orientation of the SAXS streaks for the four sets of fibres in the S_2 layers with the X-ray beam directed at 45° to both sets of cell walls. (b) Small angle scattering pattern from a *Pinus radiata* specimen with the x-ray beam directed at 45° to both sets of cell walls.

season and chemical/mechanical treatment. Given the dual loading capability of the instrument (axial and transverse), it is also possible to investigate the effects of axial loading on transverse properties and of transverse loading on axial properties.

5.2. USDA—single fibre testing

The adequate gripping of fibres is also a problem if one wants an accurate measure of strain on a small gauge length. The ability to both view fibres at the microscopic level and test them under environmental

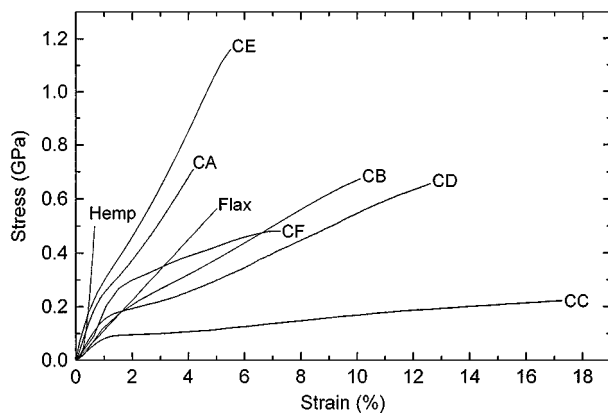


Figure 5 Stress strain curves for CA (Cordenka EHM), CB (Cordenka 1840), CC (Enka Viscose), CD (Cordenka 700) and CE (Lyocell) regenerated cellulose fibres and Steam Exploded Flax and Field Retted Hemp fibres.

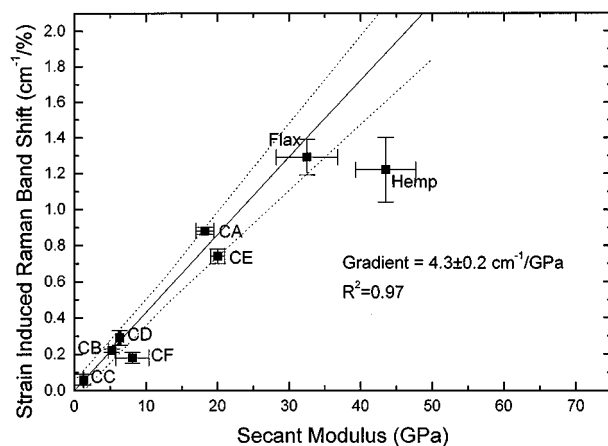


Figure 6 Relationship between Raman shift strain rate and modulus of cellulose fibres. Dotted lines indicate the upper and lower 95% confidence bands.

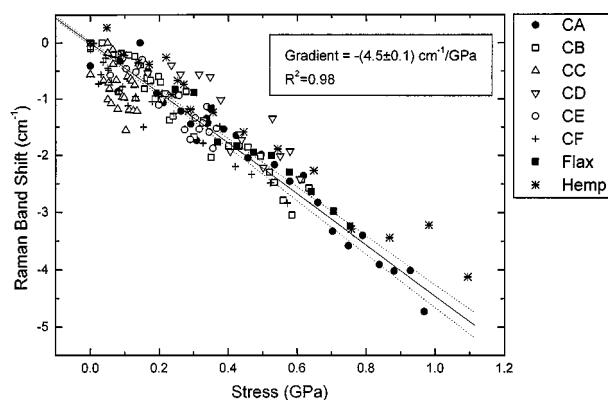


Figure 7 The stress-dependant band shifts for a number of cellulose fibres. Dotted lines indicate the 95% confidence bands.

conditions also poses problems for workers in the natural fibre community.

Les Groom of the USDA has also been investigating the mechanical properties of single wood fibres using novel testing procedures. The first researchers to determine wood fibre mechanical properties relied on two primary tensile techniques: gripping individual fibres in miniature friction-enhanced grips or adhering individual fibres to tabs and gripping the tabs [29, 42, 43].

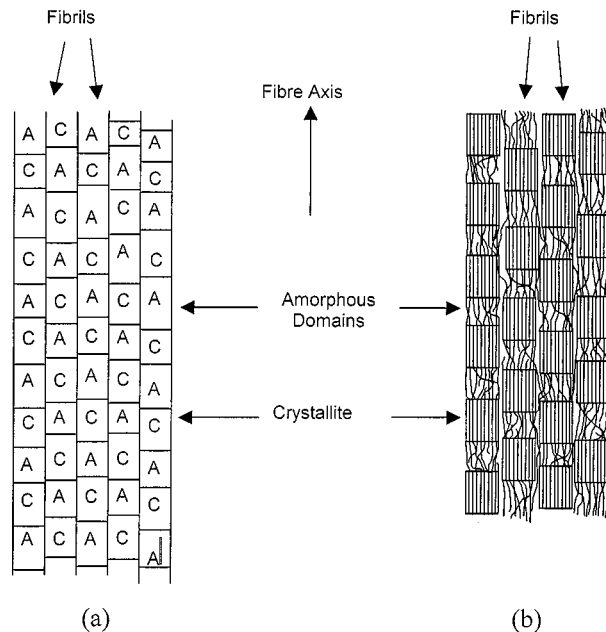


Figure 8 Schematic diagram of (a) the modified series model; (b) possible physical structure of a semi-crystalline cellulose fibre.

These techniques were tedious, slow, and often resulted in failures at or very near the grips. Kersavage [40] introduced the idea of placing epoxy droplets on the ends of individual wood fibres and applying a tensile load to across the droplets, essentially forming a ball-and-socket type gripping assembly. Kersavage [40] found that the epoxy droplets minimized stress concentrations on the fibre and reduced the fraction failed at or near the grips. This apparatus was further modified by Groom *et al.* [44] so as to increase the number of samples that can be tested each day as well as minimize grip and crosshead deflections (Fig. 12).

Failure mechanisms were characterized by observation under the environmental scanning electron microscope (ESEM). Successive 640 by 480 pixel images of fibres under stress in the ESEM chamber were digitally captured and analysed by a digital image correlation (DIC) algorithm. Conditions in the ESEM chamber were an approximate pressure of 6 Torr, 21°C, and a fibre EMC of 8.5%. The DIC algorithm was run on a Silicon Graphics workstation with a sub-pixel precision of ± 0.1 pixel. Specifics of the ESEM settings and DIC algorithm can be found in [45].

Cross-sectional determination of failed fibre sections are accomplished with a confocal scanning laser microscope (CSLM). The microscope used at this lab include a BioRad model MRC 600 and more recently a BioRad model MRC1000. Refined fibres generally do not need additional staining due to the natural biofluorescence of the remaining lignin. Chemically generated fibres with low lignin contents generally require supplemental staining. Specifics regarding staining wood fibres for fluorescence can be found in [45, 46].

Fig. 13 shows a strain map of a black spruce fibre generated from digital images taken under stress in the ESEM chamber and calculated with DIC [45, 47, 49, 94]. It was found that localized longitudinal strains in the proximity of pits were orders of magnitude greater

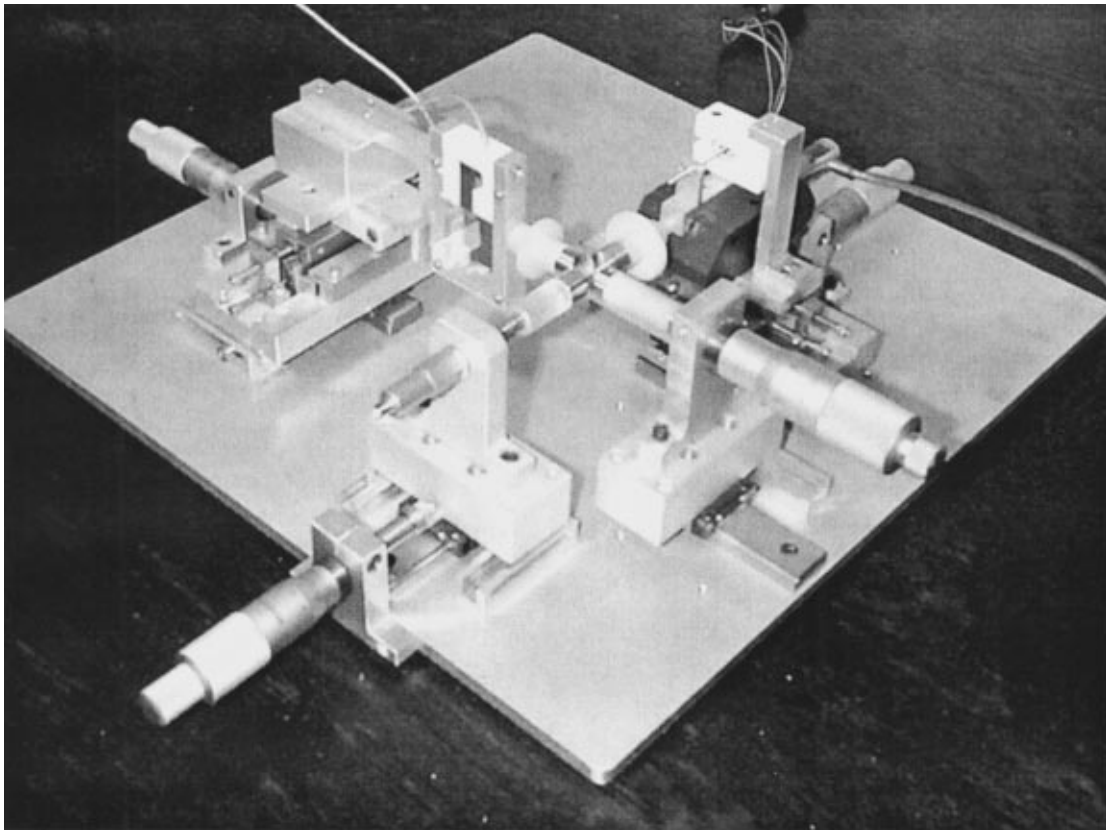


Figure 9 The single fibre test instrument.

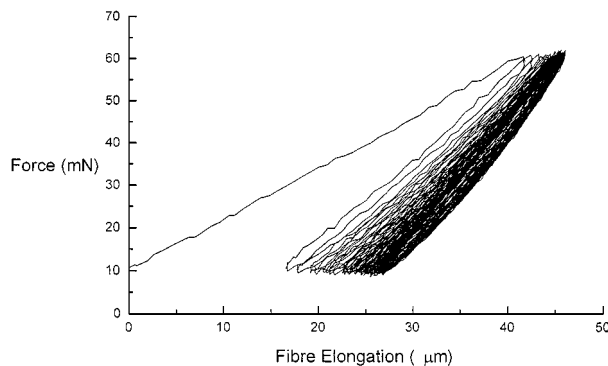


Figure 10 Typical cyclic axial force-elongation data [38].

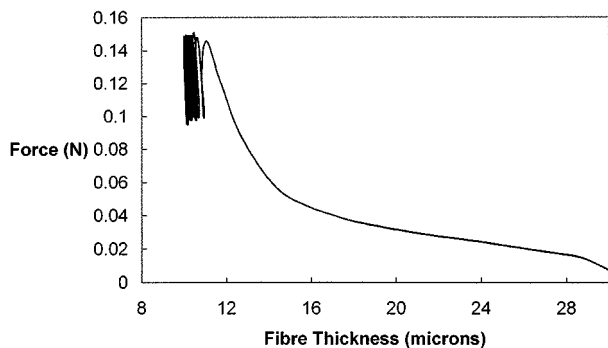


Figure 11 Typical cyclic transverse force-elongation data.

than cell wall material that was defect-free or contained microcompressions. This was corroborated by physical observations of fibres in the ESEM chamber, with almost all fibres failing in tension within the immediate vicinity of pits.

Determination of fibre mechanical properties for virgin wood fibres is compounded by the inherent variability of wood. In an attempt to quantify these variations as well as to establish some sort of representative value for virgin loblolly pine fibres, a series of tensile tests of macerated fibres was conducted [50–52]. Results of these investigations are summarized in Fig. 14 and show that there exists a strong relationship between distance from the pith and mechanical properties. The magnitude of this effect is not constant throughout the height of the tree, with the greatest effect of juvenility on fibre mechanical properties at stump height and in the live crown.

Current research is now investigating the effect of refining on the physical, chemical, and mechanical properties of fibres for the manufacture of medium density fibreboard (MDF) [53–57]. These properties will then be related to the structural performance of the final MDF product. A preliminary examination of refining pressures (4, 8, and 12 bar) indicates that increasing refining pressures result in diminished fibre mechanical properties (Fig. 15). The effect on MDF panel mechanical properties are a bit more complex due the plasticisation and redeposition of lignin on the fibre surfaces. This research is being expanded to include pressures ranging from 2 to 18 bar and from fibre juvenility and maturity. Data from these studies will allow us to optimise refiner conditions, maximize MDF properties, and adapt to increasing levels of juvenile fractions.

6. Chemical modification of fibres

When it comes to using natural fibres as reinforcement in composite materials many problems occur at the

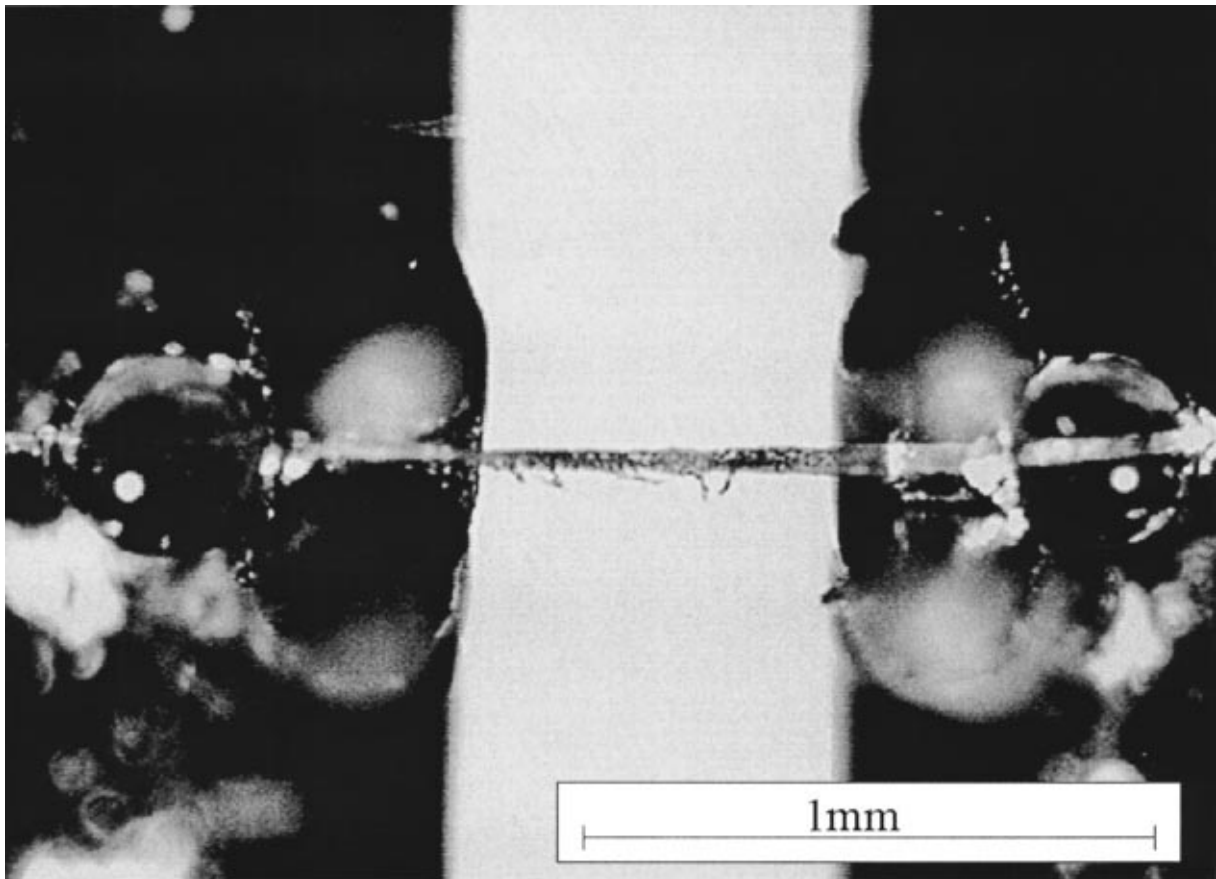


Figure 12 Tensile testing apparatus for determination of mechanical properties of individual wood fibers. Note epoxy droplets on fiber and grips.

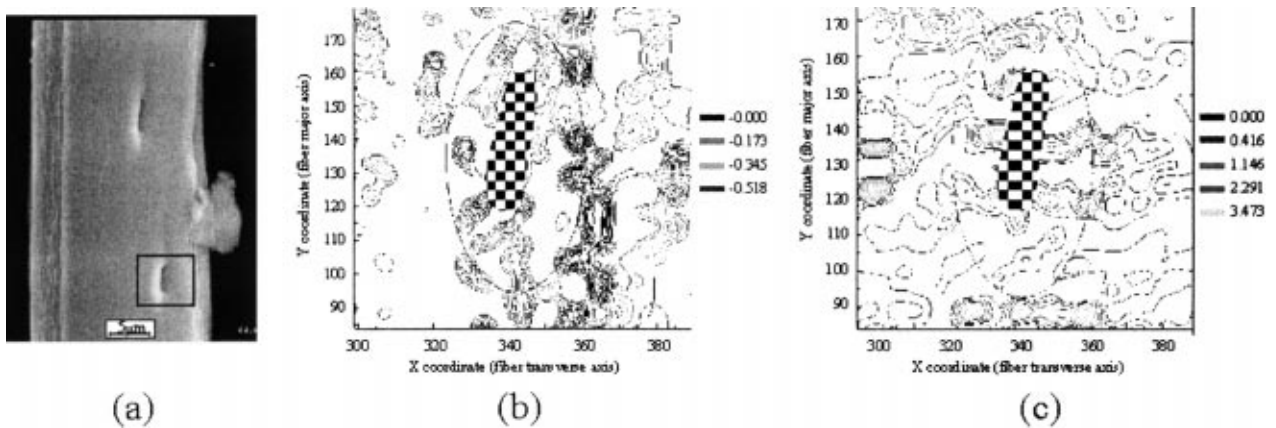


Figure 13 A black spruce fiber under stress in the ESEM, where (a) digital image of the strained fiber and (b) the corresponding transverse strain map of the lower pit, and (c) the corresponding longitudinal strain map of the lower pit.

interface due to imperfect bonding. Therefore modification of the fibres by chemical treatment is one large area of research that a number of workers are currently investigating to improve compatibility. The modification of the fibres can both increase or decrease the strength of the fibres, and thus an understanding of what occurs structurally is of paramount importance.

6.1. CICY Mexico—chemical modification of fibres

Pedro Herera-Franco and Gonzalo Escamilla, CICY, Mexico have been looking at this problem for some time. They have found that the compatibility can be im-

proved by grafting a matrix-compatible polymer onto the fiber surface. Initiation by free radicals is one of the most common methods used for the grafting of vinylic monomers onto cellulose [58]. These free radicals are produced as a result of a reaction of the cellulosic chain in a redox system. In this reaction, oxidation of the anhydroglucose units occur along the cellulosic chains and macrocellulosic radicals are generated on the surface of the fiber. These reactions modify the properties of the fiber, and since one of the roles of the cellulose fibers in composites is to give stiffness and strength to the polymeric matrix, the mechanical properties of henequen (*Agave fourcoides*) cellulose fibers grafted with methyl methacrylate (MMA) has been examined by this group.

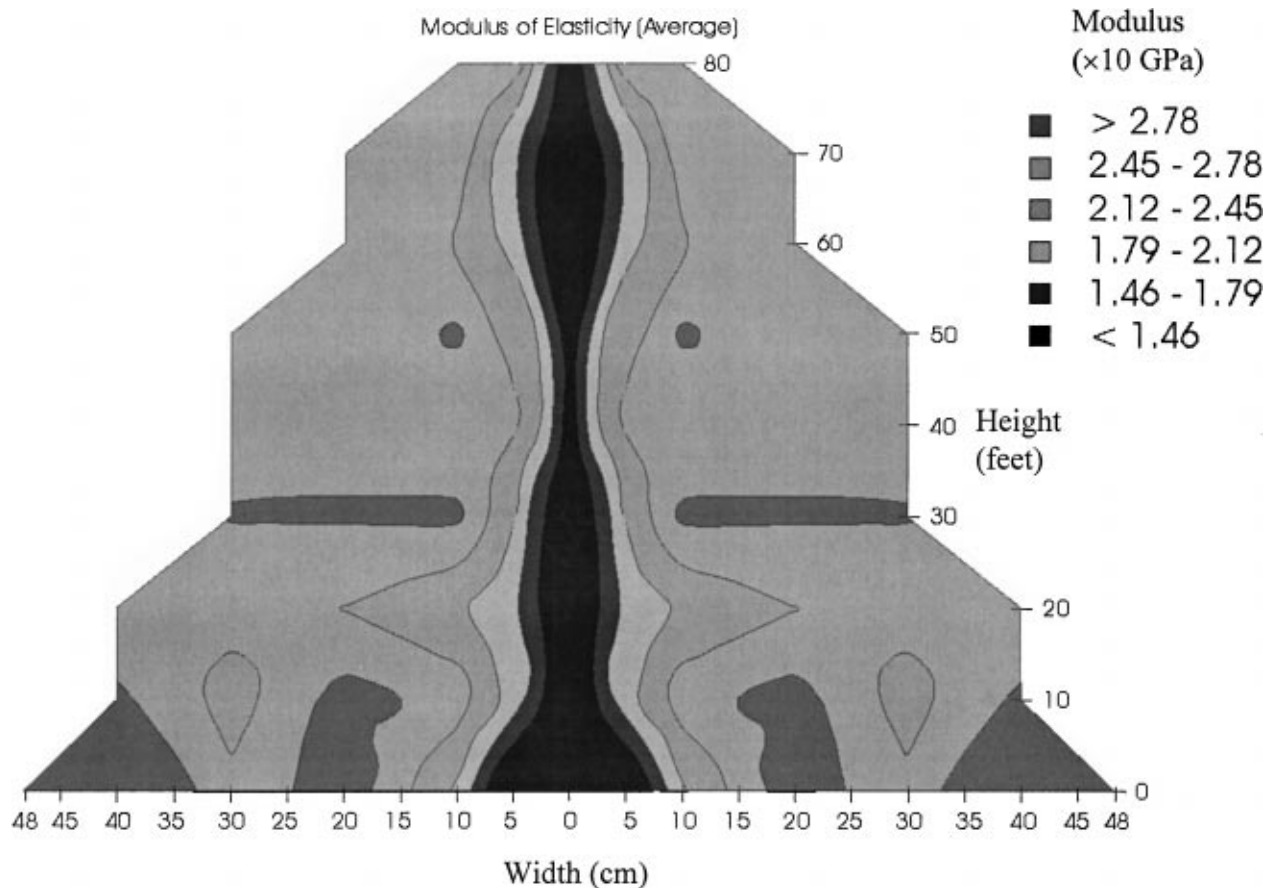


Figure 14 Map of loblolly pine fiber modulus of elasticity shown as a function of location within a tree.

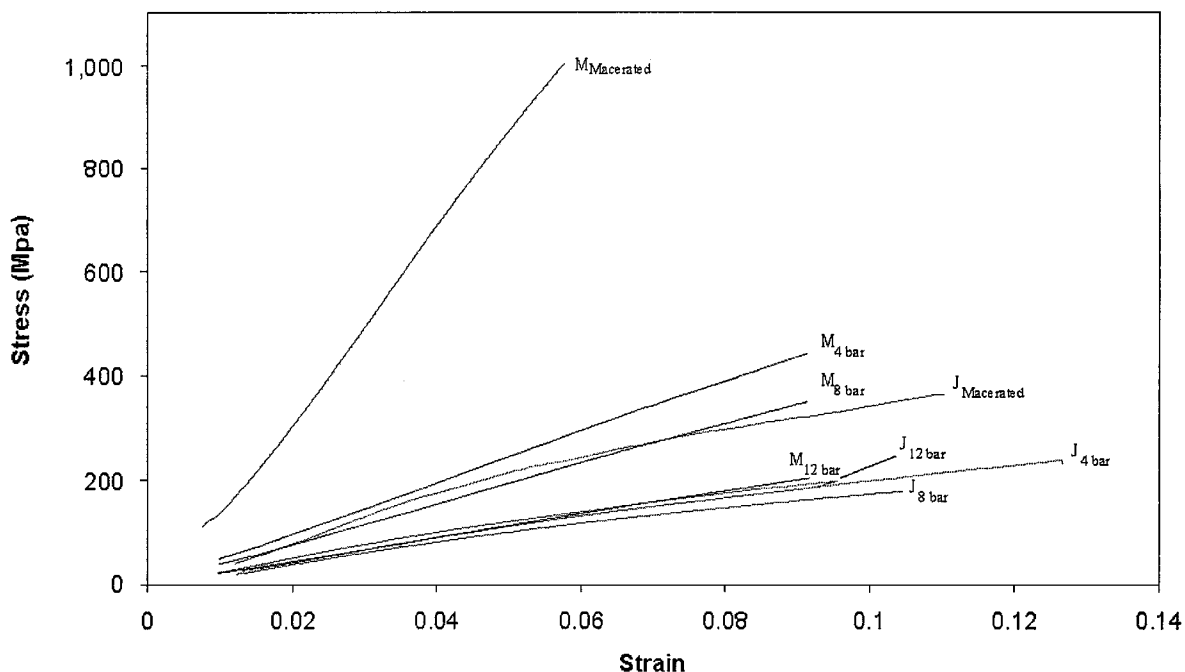


Figure 15 Stress-strain curves of juvenile and mature fibers that have either been macerated or refiner-generated, where $M_{macerated}$ = macerated mature fibers, M_{4bar} = mature fibers refined at 4 bar, M_{8bar} = mature fibers refined at 8 bar, M_{12bar} = mature fibers refined at 12 bar, $J_{macerated}$ = macerated juvenile fibers, J_{4bar} = juvenile fibers refined at 4 bar, J_{8bar} = juvenile fibers refined at 8 bar, and J_{12bar} = juvenile fibers refined at 12 bar.

For increasing initiator concentration without any monomer present in the reaction, a decrease of the elastic modulus, the ultimate deformation and the molecular weight is observed, and the largest decrease corresponds to the 10 mmol/l initiator concentration

(Table III). The tensile strength increases but for concentrations above 10%, it decreases again. This decrease of properties can be attributed to both, the oxidation of cellulose and chain rupture, because of the initiator and the acidity of the reaction medium [59]. On

TABLE III Effect of the initiator concentration on the mechanical properties of the cellulose fibre

CAN (mmol/l)	Crystallinity (%)	Molecular weight (Dalton)	Elastic modulus (GPa)	Tensile strength (MPa)	Ultimate deformation (%)
0	38	108 100	1.63 ± 0.42	188 ± 31	20 ± 5
2	45	101 600	1.34 ± 0.48	248 ± 37	15 ± 5
6	48	93 500	1.36 ± 0.46	209 ± 54	16 ± 4
10	51	67 900	0.86 ± 0.31	119 ± 26	12 ± 3

TABLE IV The effect of the initiator concentration on the mechanical properties of MMA-grafted cellulose fibres

CAN (mmol/l)	Grafted polymer (%)	Crystallinity (%)		Mw of PMMA (Dalton)	Elastic modulus (GPa)	Tensile strength (MPa)	Ultimate deformation (%)
		A	B				
0	—		38	—	1.63 ± 0.43	188 ± 31	20 ± 5
2	46.4	27	50	196 000	1.26 ± 0.52	99 ± 35	10 ± 3
4	47.2	25	47	143 000	1.41 ± 0.62	125 ± 32	8 ± 4
6	47.2	28	53	116 000	1.37 ± 0.35	123 ± 43	12 ± 5
8	46.1	28	51	92 000	1.65 ± 0.59	113 ± 31	8 ± 3

A: calculation is based on the grafted fibre (cellulose + PMMA).

B: calculation is based on weight (%) of cellulose in the grafted fibre.

TABLE V Effect of the grafting amount (%) of a polymer (PMMA) on the properties of cellulose

Grafted polymer (%)	Crystallinity (%)		Molecular weight of PMMA (Dalton)	Elastic modulus (GPa)	Tensile strength (MPa)	Ultimate deformation (%)
	A	B				
0	—	48	—	1.36 ± 0.46	209 ± 54	16 ± 4
31.7	40	59	58 000	0.80 ± 0.34	97 ± 30	15 ± 5
47.6	28	53	116 000	1.16 ± 0.47	145 ± 50	9 ± 2
54.4	23	59	305 000	1.02 ± 0.39	92 ± 32	11 ± 2

the other hand, the crystallinity of the fibers increases with increasing initiator concentration.

When the reaction is carried out in the presence of a monomer (MMA) the oxidation or depolymerisation is lower than in the case of cellulose alone. In this case the macro-cellulose radicals generated by the initiator are used to carry out the graft copolymerisation of the polymer and the degradation of the cellulose is reduced. As shown in Table IV, the elastic modulus is not affected significantly, but the tensile strength and the ultimate deformation are reduced. The grafting of an amorphous polymer (PMMA) onto the cellulose results in a reduction of the crystallinity degree of the grafted fibre. The grafted fibre has a crystallinity of 25–28% and, after correcting based on the amount of cellulose determined in the copolymer, the value of the crystallinity of the cellulose is approximately 47–53%. Such increase indicates that the reaction takes place in the amorphous zone of the fibre.

The effect of the initiator concentration on the mechanical properties of MMA-grafted cellulose fibers is also noted. An increase in the amount of grafted PMMA onto the fibre (see Table V) results in a decrease of the crystallinity, because a larger amount of an amorphous polymer is present on the grafted fibre. There is a decrease of the elastic modulus and the tensile strength, however it would be difficult to say that such dispersion of values is due to the presence of the PMMA rather than the degradation produced by the reaction itself.

6.2. Bath, UK—chemical modification

Other techniques that have been investigated have been alkalisation and acetylation. Martin Ansell and Leonard Mwaikambo of Bath University have been looking at these techniques to improve the quality of fibres from plants. The fibre types they have investigated have been hemp, sisal, jute and kapok. These researchers, and co-workers, have developed a number of composite materials based on plant fibres with synthetic or natural polymer matrices. Composite systems include straw-polyester [60], jute-polyester [9, 61] sisal-epoxy [62, 63], and sisal-cashew nutshell liquid (CNSL) [4], cotton/kapok-polyester [64] and cotton/kapok-polypropylene [65]. Current work at the University of Bath concerns the surface treatment of hemp, sisal, jute and kapok fibres for the reinforcement of plant fibre composites. There is a considerable amount of debate in the literature on the benefits of treatment of plant fibres by alkalisation and acetylation and the findings of recent work at Bath [66] are thus summarised.

Table VI summarises the property ranking of fibres when subjected to chemical treatment by alkalisation and acetylation. The fibre with the highest ranking is ranked 4 and the lowest is ranked 1.

Alkalisation of plant fibres changes the surface topography of the fibres and their crystallographic structure. However, care must be exercised in selecting the concentration of caustic soda for alkalisation, as results show that some fibres at high NaOH concentrations

TABLE VI Property ranking of hemp, sisal, jute and kapok fibres

Technique	Treatment	Hemp	Sisal	Jute	Kapok
Crystallinity index (CI) (WAXRD) 1st Exothermic peak (DSC)	Alkalisiation	Highest (CI) 4	2	3	Lowest (CI) 1
	Alkalisiation	Strongest peak 4	Irregular	Irregular	Irregular
	Acetylation without acid catalyst	Strongest peak 4	2	3	Weakest peak 1
	Acetylation with acid catalyst	Strongest peak 4	Irregular	3	Irregular
Reaction to chemicals (FT-IR)	Alkalisiation	Least reactive 1	2	3	Most reactive 4
	Acetylation without acid catalyst	Least reactive 1	2	3	Most reactive 4
	Acetylation with acid catalyst	Least reactive 1	2	3	Most reactive 4

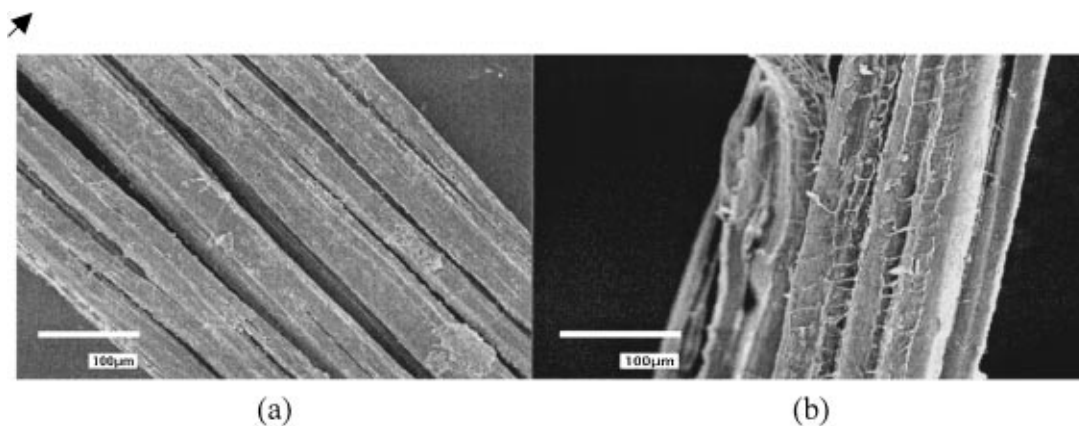


Figure 16 Hemp fibre (a) untreated and (b) 8% NaOH treated.

have reduced thermal resistance as elucidated by the Differential Scanning Calorimetry (DSC) method. It is believed that the increase in the crystallinity index measured by Wide Angle X-ray Scattering (WAXS) is in actual fact an increase in the order of the crystallite packing rather than an increase in the intrinsic crystallinity. A high crystallinity index is likely to result in stiff, strong fibres of interest in the formation of plant fibre composites. It is essential, therefore, to use several complementary techniques when studying the fine structure of plant fibres to confirm trends. The application of the DSC technique as well as the WAXS method probably gives a better analysis of the fine structure of the plant fibres than the WAXS method alone. The removal of surface impurities on plant fibres is advantageous for fibre-matrix adhesion as it facilitates both mechanical interlocking and the bonding reaction due to the exposure of the hydroxyl groups to chemicals such as resins and dyes. By observing the first exothermic peak (DSC) which is a measure of the cellulose thermal characteristics, hemp fibre shows the highest stability after acetylation followed by jute, sisal and kapok fibres. This implies that acetylation does not result in the degradation of the crystalline cellulose.

Fourier Transform Infrared (FT-IR) spectroscopy has provided additional information on the reactivity of fibres following treatment by alkalisiation and acetylation. From these results it can be concluded that sisal, jute and kapok fibres are suitable for grafting chemical structures onto their main structure as evidenced by the presence of the peak intensity of the acetylated fibres at the 1740 cm^{-1} band and its dis-

appearance on alkalisiation. Hemp fibre might not be as suitable in this case. However, SEM results indicate that after chemical treatment, at low concentration, all the fibres except kapok possess rougher surfaces, which will enhance mechanical interlocking with resins. The untreated hemp fibres are in separated bundles with a smooth surface (Fig. 16a) while alkalisied fibres (Fig. 16b) have a rough surface with more separation of the individual fibres. Untreated sisal (Fig. 17a) have joined fibre cells while alkali treated sisal fibres (Fig. 17b) show split individual fibres with more scooped individual cells implying that a removal of surface materials have taken place. Fig. 18 shows untreated and alkalisied jute fibres in which the untreated fibre is smooth with fibre bundles being held together in a matrix of waxy materials (Fig. 18a). Fig. 19a shows untreated kapok fibres while Fig. 19b shows kapok fibres alkalisied with 8% NaOH and Fig. 19c is that of 400% NaOH treated kapok fibres. It is observed that alkalisiation at low caustic soda concentration has no noticeable effect on the surface of kapok fibre while high concentration results in grooved serrated surfaces (Fig. 19c).

These alkalisiation effects on natural fibres are of particular importance for fibre - matrix adhesion and the creation of high fibre surface area required for the optimisation of fibre - resin reinforcement. The modification of cellulose fibres, therefore, develops into changes in morphology and increase in hydroxyl groups. These changes will effectively result in improved surface tension, wetting ability, swelling, adhesion and compatibility with polymeric materials [85].

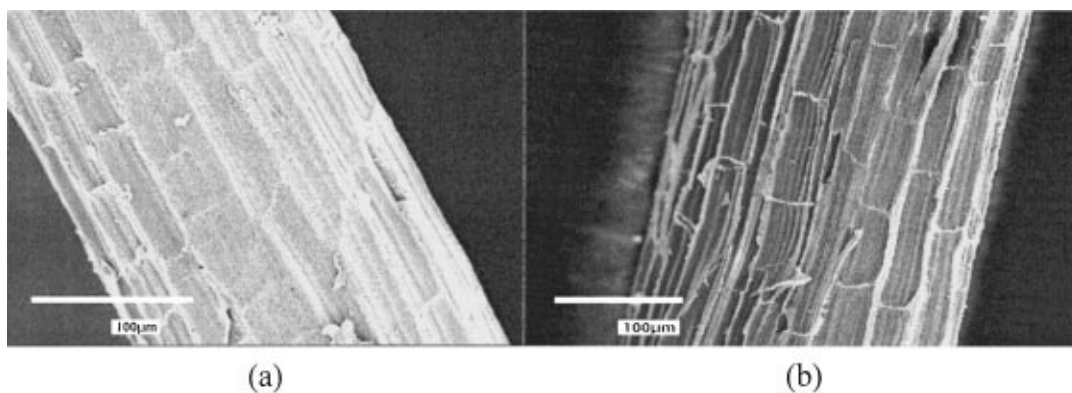


Figure 17 Sisal fibre (a) untreated (b) 8% NaOH treated.

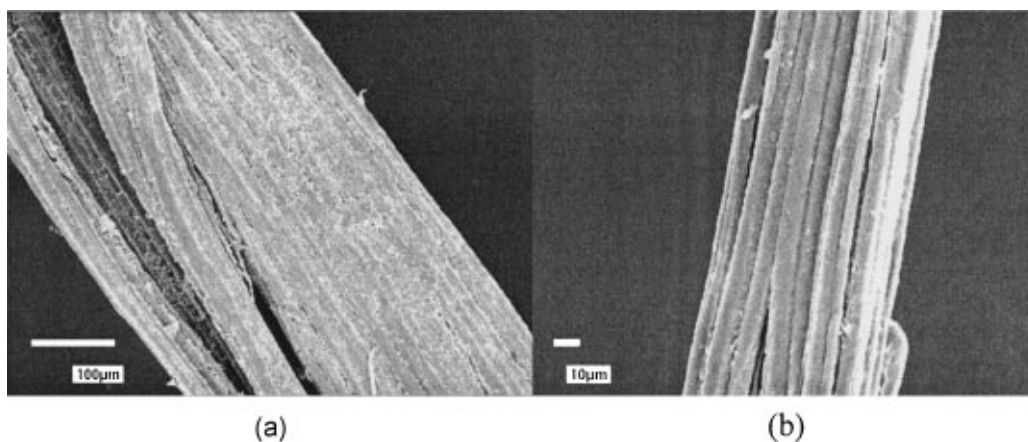


Figure 18 Jute fibre (a) untreated and (b) 8% NaOH treated.

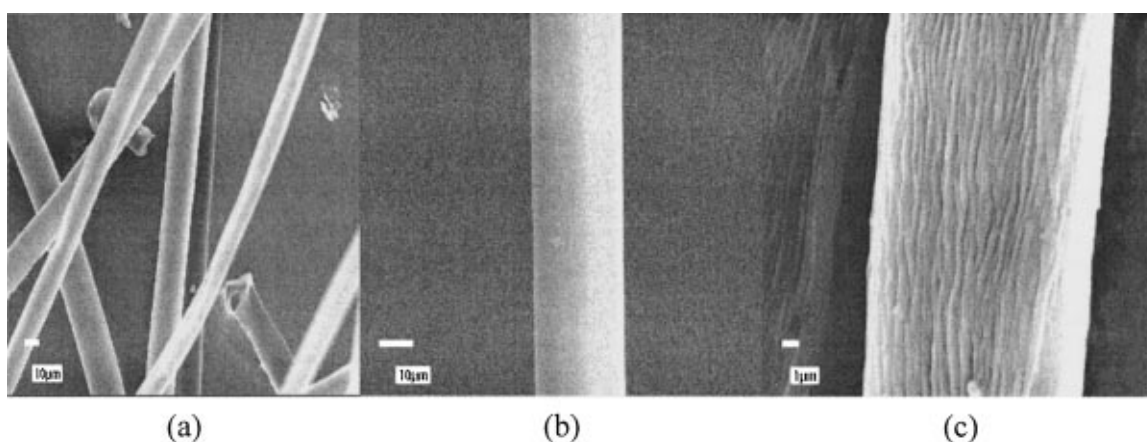


Figure 19 Kapok fibre (a) untreated (b) 8% NaOH and (c) 400% NaOH treated.

However, high concentration of caustic soda result in grooved serrated surfaces for kapok. Chemical treatment will produce composites with improved mechanical properties. However, though Table VI does not give any general trend, hemp appears to have the highest crystallinity index and thermal stability when alkalisied and acetylated with and without acid catalyst followed by jute, sisal and then kapok fibres. Kapok fibre has the highest reaction affinity to chemicals followed by jute, sisal and hemp fibres.

The high reactivity of kapok fibre during alkalisation and acetylation is due to the high content of semi-crystalline and amorphous materials such as hemicellulose and lignin and the presence of the reactive hydroxyl

groups on the fibre surface and in the amorphous region. Fibres with high crystallinity index, hence low amorphous regions, such as hemp exhibit least reactivity because they are highly crystalline thus rendering fewer hydroxyl groups available for reactions with interacting chemicals. This also explains why the first exothermic peak temperature (DSC) is lower in fibres with the highest amount of amorphous cellulose (kapok fibre) than those with the least amount of amorphous cellulose such as hemp. The removal of hydroxyl groups on plant fibres by acetylation (FT-IR) will make the fibres non-polar. The implication of this result is that the fibres become unable to react with polar resins such as cashew nut shell liquid (CNSL) or epoxies. The fibres

will therefore only bind by the mechanical interlocking adhesion mechanism.

On the basis of this work on thermal characterisation of hemp, sisal, jute and kapok, work is now proceeding on composite systems based on hemp, sisal and jute fibres in matrices of polymerised CNSL, epoxy resin and polyester resin.

6.3. Imperial College—chemically treated flax fibre composites

Flax fibres can be thought of as biological composites. The cell wall of flax is constituted of a middle lamella at the outside, a primary wall, a secondary wall and a lumen. The primary and secondary walls of flax fibres show different mechanical behaviour due to their different chemical composition and morphology. Any alteration of the characteristics of the cell wall, either chemical or morphological, has an effect on the mechanical properties of the fibre. Surface treatments as well as other factors like crop maturity and retting are able to cause changes to the cell wall characteristics. Caroline Baillie and Nicholas Zafeiropoulos from Imperial College, London are involved in research to modify the interface between flax fibres and a variety of matrices. In Table VII the average tensile strengths of green flax (flax as received from the fields), dew retted (green flax that has undergone a bacterial treatment on the fields) and Duralin (flax treated by a method developed by CERES BV, Netherlands, which involves the depolymerisation of lignin and hemicelluloses into lower molecular aldehyde and phenolic functionalities followed by a subsequent curing that hydrophobises the fibre surface) at different gauge lengths are shown [67]. An overall trend of the results is that for 3.5, 6 and 8 mm gauge lengths the value of the average tensile strength is higher for Duralin than for dew-retted and higher for dew-retted than for green flax. The single fibre strength is certainly much higher than the fibre bundle (elementary fibre) strength. The reason for this difference is that the fibre bundle fails within the hemicellulose and pectin layers that connect the single fibres together.

From the early development of composite materials the optimisation of the interface has been of pivotal importance. In classical man made fibre composites, i.e. glass, carbon, aramid, etc., various methods of modifying the fibre surface, like silane sizings, electrochemical oxidation, etc., have been found to be very successful in controlling the interface. However, natural fibres are quite different than man made fibres. Natural fibres are

TABLE VIII Average shear strength of flax fibres in various matrices by the pull out test

Model composite	Average shear Strength τ (MPa)
Green flax/polyester	17.1
Duralin/polyester	11.7
Duralin/epoxy	23.2
Green/LDPE	5.4
Duralin/LDPE	4.4
Dew retted/HDPE	9.1
Dew retted/LDPE	5.5
Dew retted/iPP	10.6
Dew retted/MAPP	11.4
Duralin/HDPE	10.1
Duralin/LDPE	6.2

strongly hydrophilic materials and moisture absorption leads to a significant deterioration of their mechanical properties. Furthermore, most polymers are hydrophobic and due to this divergent behaviour the interface in natural fibre composites is rather poor. The interface in flax fibre composites has been assessed by the pull out test [68, 69]. The following polymers are used as potential matrices: unsaturated polyester, epoxy, low density polyethylene (LDPE), high density polyethylene (HDPE), isotactic polypropylene (iPP) and maleic anhydride modified polypropylene (MAPP). The results are shown in Table VIII. It is worth noting that green flax outperformed dew retted flax when polyester was used as a matrix and that MAPP did not significantly increase the interfacial shear strength in comparison with iPP. The examination of the pull out force versus displacement curves indicated a brittle fracture mixed mode interface behaviour. From Table VIII it is clear that the best adhesion, from the greatest average interfacial shear stress, is the Duralin/epoxy system, and the worst is green flax and the low density polyethylene combination.

Normal methods of modifying the interface are usually not applicable in natural fibres for many reasons, cost being the most important. Natural fibres cannot compete in terms of strength with man-made fibres, but their main advantage is their low cost. Therefore a cheap method is needed to enhance the interface in natural fibre composites. Current research has been focused on controlling the interface either by chemically modifying the fibre surface to make it more hydrophobic or by optimising the processing conditions. The system under study is flax fibres/isotactic polypropylene (iPP). Isotactic polypropylene is a semicrystalline polymer, and in the case of such polymeric matrices transcrystallinity develops in the vicinity of the fibre surface, and has been found to affect the interface. Flax fibres have been shown to induce transcrystallinity with iPP, HDPE and MAPP [70]. Transcrystallinity was found to be affected by the type of fibre used. Four different types of flax were studied. Green flax, dew retted flax, stearic acid treated flax and Duralin treated flax. All the fibres induce a transcrystalline layer with iPP, but only dew retted flax is able to induce such a layer with HDPE and MAPP. The thickness of transcrystallinity varies for the different types of flax with dew retted flax giving the most uniform layer. The morphology of the

TABLE VII Comparison of the strength of Duralin, green and dew-retted flax fibres for different gauge lengths

Gauge length (mm)	Type of fibre	Average strength (MPa)		
		Dew-retted	Duralin	Green
3.5	single fibre	821.9	1154.1	446.1
3.5	bundle	109.7	161.6	124.5
6	single fibre	898.6	905.3	568.6
8	single fibre	765.8	826.36	667.56
8	bundle	156.8	151.7	388.4

TABLE IX Dependence of fibre critical length and τ values (Kelly-Tyson model) upon the T_c layer thickness

System	Transcrystalline layer thickness (μm)	Mean fragment length (μm)	Critical length (μm)	τ value (MPa)
iPP/dew retted flax	—	889	1185	12.75
iPP/dew retted flax ($T_c = 145^\circ\text{C}$)	50 ± 10	533	711	23.05
iPP/dew retted flax ($T_c = 145^\circ\text{C}$)	100 ± 10	533	711	23.05
iPP/dew retted flax ($T_c = 140^\circ\text{C}$)	50 ± 10	533	711	23.05

TABLE X Tensile strength for treated and untreated dew retted flax (Mean values (in MPa) with standard deviation)

Strength Untreated dew retted flax σ (MPa)	Gauge length	Strength after acetylation			
		1% weight gain	4.7% weight gain	10% weight gain	15.3% weight gain
906.4 ± 246.3	5 mm	879.6 ± 253.2	840.6 ± 234.3	851.4 ± 127.9	700.2 ± 199.2
736.8 ± 208.6	8 mm	690.9 ± 290.1	700.2 ± 267.3	683.2 ± 200.3	595.4 ± 212.7
602.6 ± 198.4	10 mm	605.3 ± 187.3	613.6 ± 143.2	600.7 ± 189.3	519.6 ± 143.9
		Strength after stearic acid treatment at 105°C			
906.4 ± 246.3	5 mm	0.1% weight gain 863.2 ± 223.7	0.16% weight gain 807.9 ± 153.7	0.24% weight gain 730.7 ± 150.5	0.30% weight gain 674.2 ± 124.2
736.8 ± 208.6	8 mm	700.1 ± 118.3	687.3 ± 176.2	620.4 ± 98.6	580.7 ± 190.3
602.6 ± 198.4	10 mm	591.2 ± 167.4	549.1 ± 117.2	498.2 ± 100.3	387.8 ± 230.3

TABLE XI Tensile strength for treated and untreated green flax (Mean values (in MPa) with standard deviation)

Untreated green flax σ (MPa)	Gauge length	Strength after acetylation			
		1.5% weight gain	5.4% weight gain	10.6% weight gain	16.1% weight gain
678.9 ± 216.2	5 mm	650.2 ± 196.4	670.4 ± 153.9	700.5 ± 149.3	720.3 ± 153.9
523.7 ± 175.3	8 mm	510.7 ± 145.6	570.3 ± 178.4	580.5 ± 198.3	600.1 ± 132.4
468.3 ± 211.6	10 mm	490.2 ± 187.5	497.1 ± 157.3	510.2 ± 211.4	523.4 ± 120.4
		Strength after stearic acid treatment at 105°C			
678.9 ± 216.2	5 mm	0.12% weight gain 669.3 ± 178.3	0.19% weight gain 670.2 ± 159.3	0.27% weight gain 600.7 ± 166.8	0.31% weight gain 567.3 ± 221.1
523.7 ± 175.3	8 mm	500.5 ± 169.4	507.3 ± 187.2	482.6 ± 198.5	440.6 ± 143.7
468.3 ± 211.6	10 mm	470.1 ± 201.4	476.9 ± 136.7	437.9 ± 185.9	401.4 ± 190

transcrystallites was found to be the same as of the bulk spherulites (α type-monoclinic).

The effect of transcrystallinity upon the interface has been assessed using the single fibre fragmentation test. The results are shown in Table IX [71]. There is a significant improvement of the interface when transcrystallinity is present as shown by the sharp decrease of the critical length. The thickness of the transcrystalline layer is not found to affect the interface. However, in the transcrystalline layer there is an extensive crazing around the zone of the fibre break. This phenomenon has been termed ‘treeing failure’ [72]. The damage consists of an interlamellar crack within the transcrystalline zone, which eventually propagates through the spherulites in the matrix. This failure mode suggests that the presence of transcrystallinity can also increase energy absorption apart from the interfacial strength. Two more methods have been employed to promote a better interface; acetylation and stearic acid sizing. Acetylation is performed following the method by Rowell *et al.* [73]. Stearic acid was employed following a novel method from the vapour phase [74]. The aim of both treatments is to react the hydroxyl groups of the

fibre with acetyl groups, in the case of acetylation, or, in the case of stearic acid with stearic acid groups and subsequently to hydrophobise the fibre’s surface yielding a better compatibility with polypropylene. One of the key questions is what kind of effect upon the fibre mechanical properties this treatment has when it is applied on the fibres. In Tables X and XI the effect of acetylation and stearic acid treatments upon the fibre strength is shown [74]. Acetylation does not affect significantly the dew retted flax fibre strength for small reaction times. For large reaction times a reduction of fibre strength occurs. For green flax, acetylation is found to cause a slight increase of the fibre strength. The reason for this increase may be the fact that some of the more amorphous constituents of the fibre, especially pectins, are removed during the treatment. Stearic acid treatment does not affect significantly the fibre strength for either green and dew retted flax at low reaction times. However, at higher reaction times there was a significant deterioration of the fibre strength for both types of flax. The effect of these treatments on the interface has been assessed using the single fibre fragmentation test. The results are shown in Tables XII and XIII [74]. It can be

TABLE XII Dependence of fibre critical length and τ values (Kelly-Tyson) upon the extent of fibre treatment for dew retted flax

System	Weight % gain	Mean fragment length (μm)	Critical length (μm)	τ value (MPa)
iPP/dew retted flax	—	889	1185	12.75
iPP/acetylated dew retted flax	4.7	800	1067	13.05
iPP/acetylated dew retted flax	10	800	1067	12.95
iPP/acetylated dew retted flax	15.4	800	1067	12.50
iPP/Stearic acid treated dew retted flax (12 hrs at 105 °C)	0.1	889	1185	12.02
iPP/Stearic acid treated dew retted flax (36 hrs at 105 °C)	0.16	800	1067	13.36
iPP/Stearic acid treated dew retted flax (90 hrs at 105 °C)	0.3	1143	1524	6.40

TABLE XIII Dependence of fibre critical length and τ values (Kelly-Tyson) upon the extent of fibre treatment for green flax

System	Weight % gain	Mean fragment length (μm)	Critical length (μm)	τ value (MPa)
iPP/green flax	—	1333	1777	6.33
iPP/Acetylated green flax	5.4	1000	1333	8.44
iPP/Acetylated green flax	10.6	889	1185	9.49
iPP/Acetylated green flax	16.3	727	969	11.61
iPP/Stearic acid treated green flax (12 hrs at 105 °C)	0.13	1143	1524	7.38
iPP/Stearic acid treated green flax (36 hrs at 105 °C)	0.19	889	1185	9.49
iPP/Stearic acid treated green flax (90 hrs at 105 °C)	0.28	1600	2133	4.57

seen that acetylation slightly improves the interface for dew retted flax and causes significant improvement for green flax. Stearic acid sizing causes an improvement of the interface only for low reaction times, while for larger reaction times there is a deterioration of the interface. From the results is evident that acetylation seems to be a potentially good method for treating flax fibres to be used as reinforcements in iPP. Stearic acid sizing is also a promising method under development.

6.4. USDA, USA—wood fibre composites

New materials derived from wood and thermoplastic polymers have attracted considerable attention in recent years. The development of this novel composite type has presented new versions of common problems, such as material handling and processing. Substantial progress has been made toward overcoming the technological problems associated with compounding and extrusion of wood-filled polyolefins. Work done by Tim Rials of the USDA (United States Department of Agriculture) has highlighted an important fundamental issue related to adhesion of these chemically dissimilar components by consistently illustrating the significance of the interface to composite performance properties. Unfortunately, knowledge of wood/polymer interfacial structure and properties has not enjoyed similar progress, and remains poorly understood. Therefore, currently extruded wood/polymer composites are incorporating 70–80 percent wood. As such, the volume fraction of the interface/interphase is greater and its impact on composite performance even more significant. The need to engineer the structure and properties of this element is crucial to further the range of

applications and markets for this emerging composite material.

Interfacial properties of wood/polymer composites are largely determined by the strength and nature of secondary interactions that are established across the phase boundary. For typical commodity polyolefins, interfacial stress transfer is therefore limited to relatively weak dispersion forces. To improve this important characteristic several methods have been investigated to introduce mechanical anchors. The use of fibre-grafted polymer chains and block copolymers as compatibilizing agents appear to offer the greatest promise, as has been demonstrated with maleic anhydride modified polypropylene (MAPP). This copolymer is capable of reacting with the hydroxy functionality of the wood surface while, according to reports [85], co-crystallizing with the polypropylene matrix. Tim Rial's research group has completed work on analogous styrene-maleic anhydride copolymers for improving the properties of wood fibre/polystyrene composites [86, 87].

Wood fibres were prepared from spruce (*Picea spp.*) by maceration with acetic acid according to standard methods. The fibres were modified by reaction with styrene-maleic anhydride (SMA) copolymers (Scientific Polymer Products) in dimethyl formamide at 90°C for three hours. Dimethyl aminopyridine was added in catalytic amounts to facilitate the esterification reaction. Three copolymers with a nominal molecular weight of 2000 g/mol were investigated that varied in their chemical composition – maleic anhydride content of 25, 33 and 50 weight percent. Surface energy of the fibres was determined using a Cahn Model 322 dynamic contact angle analyzer. A modified micro-droplet method was used to measure interfacial shear strength

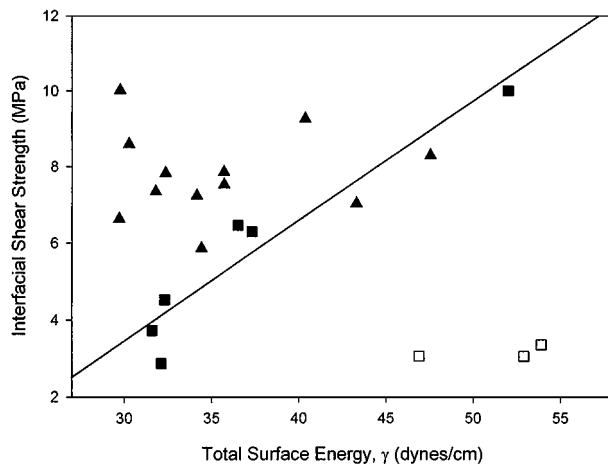


Figure 20 The variation in interfacial shear strength (ISS) with total surface energy for polystyrene with various fibres: Untreated fibres (\square), treated fibres (\blacksquare) SMA- modified fibres (\blacktriangle).

(ISS) of single fibre composites on a screw-driven, universal testing machine with a 50 g load cell. Details of the fibre modification and characterization methods employed are available in Liu, *et al.* [86].

The variation in interfacial shear strength with fibre surface energy is shown in Fig. 20 for polystyrene. Included in the graph are data for rayon, cotton and wood fibres subjected to different treatments, including thermal, washing, and acetylation [87]. The untreated, control fibres (\square) exhibit a very low ISS and relatively high surface energy. This is attributed to the presence of a weak boundary layer due to adsorbed impurities. The surface energy of the treated fibres (\blacksquare) varied from 32–52 dynes/cm[†]. A strong linear relationship, for the treated fibres, was found between the ISS and surface energy ($r^2 = 0.92$), reflecting differences in interfacial interaction for the treated fibre/polystyrene systems. Interestingly, the acetylated wood fibre exhibited the strongest adhesion to polystyrene with an ISS of 10 MPa.

The wood fibres that were modified with styrene-maleic anhydride copolymers (\blacktriangle) exhibited very different behavior. At low levels of modification (≤ 2 weight percent), the interfacial shear strength was very similar to the treated fibres discussed above. As the copolymer loading increased, however, the ISS deviated from this baseline trend and was consistently higher at a given surface energy. This presumably indicates that some degree of entanglement between the SMA copolymers and polystyrene matrix is established through diffusion and mixing. Though not explicit from Fig. 20, ISS also exhibits some dependence on chemical composition of the copolymers, decreasing as the maleic anhydride (MA) content is reduced. Copolymer effectiveness in enhancing ISS may result simply from energy-related factors like wettability or SMA/PS miscibility; however, the observed trend is inconsistent with expectations and suggests that other parameters may be influencing interfacial properties.

The relationship between chain architecture and the topology assumed by adsorbed chains has not received

[†] 1 dyne/cm $\equiv 1 \times 10^{-3}$ Nm⁻¹.

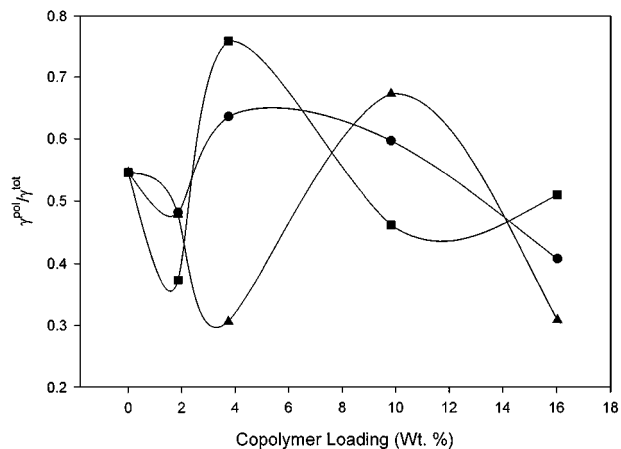


Figure 21 The effect of SMA copolymer loading on the relative contribution of the polar surface energy to the total surface energy of modified fibres: Polystyrene content = 50 (\bullet), 67 (\blacksquare), and 75 (\blacktriangle) weight percent.

much consideration, but it is potentially an important factor in achieving adequate entanglement. To address this question, the effect of copolymer content on fibre surface energy has been evaluated. Fig. 21 illustrates the effect of copolymer composition on the relative contribution of the polar component to the total surface energy at various level of modification for the SMA-modified fibres. Rather than a monotonic change to an equilibrium condition, the polar contribution fluctuates significantly as the SMA loading increases. Similar behavior has been observed for wood flour coated with polar polymers like poly(vinyl chloride) and poly(methyl methacrylate) [88]. At low loading levels ($< 5\%$) a peak minimum is observed for the three systems. The intensity of the minimum increases as the MA content of the copolymer is reduced, reflecting interaction with specific receptor sites on the fibre surface. Interestingly, the peak minimum is shifted to higher loadings for the high-PS content system. This suggests a significantly higher packing density of bound chains for this particular copolymer. At higher loading levels ($> 8\%$), the polar contribution appears to cycle around a steady decline over the range of compositions investigated. The absolute value of the parameter is dependent on the concentration of MA functionality available at the surface.

These results provide some insight into the dependence of fibre surface structure and topology on the chemical composition of the copolymers. This viewpoint also allows speculation regarding the observed behavior as it relates to copolymer efficiency as a compatibilizing agent. The high functionality copolymers do not achieve a very high packing level that leads to more dangling chains for entanglement. As the MA content is lowered, a more highly ordered surface develops that restricts interaction with the polystyrene matrix. Although much more work is needed to confirm this theory, surface structure in copolymer-modified fibres appears to be an important consideration for optimal performance.

7. High modulus cellulose fibres

One of the major problems of natural cellulose fibres such as flax and hemp is that the crystal modulus of

cellulose never achieved due to the presence of defects. These defects not only reduce the modulus but also cause anisotropy in the resulting composite material. Another problem is the ability to achieve good reinforcement with low volume fraction, and higher volume fractions are limited by aspect ratio. Some cellulose fibres produced by bacterial or animal sources overcome these problems and this section describes some research being conducted in this area.

7.1. CERMAV-CNRS, France—cellulose whisker composites

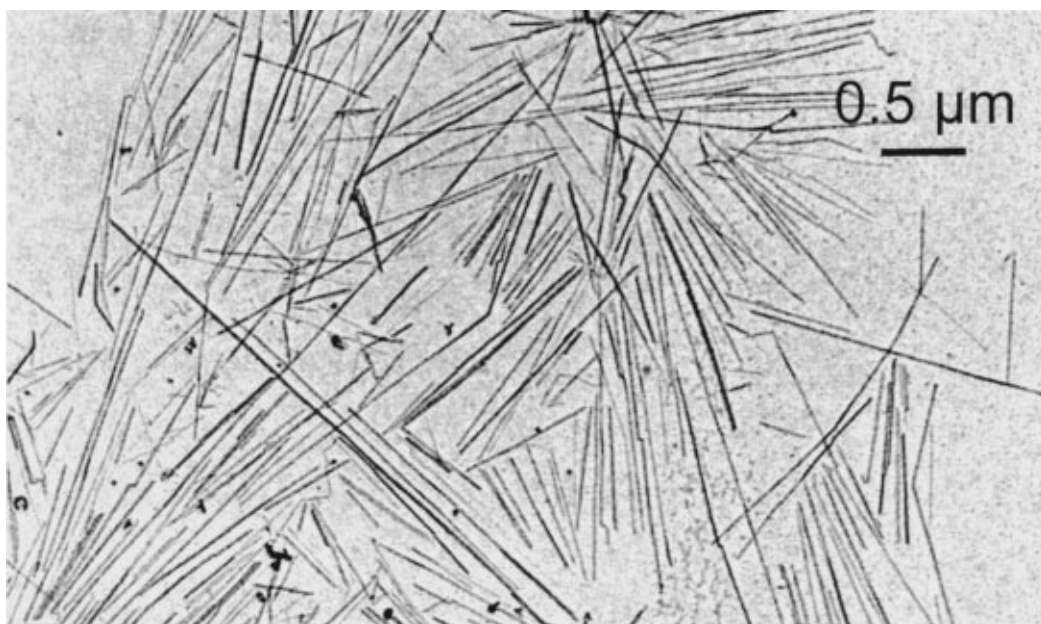
The former are being looked at by Alain Dufresne, CERMAV-CNRS, France. He has been looking at

whiskers obtained from a variety of natural and living sources. He says that lignocellulosic fillers offer attractive properties, but are used only to a limited extent in industrial practice due to their inherent hydrophilic nature and the non-polar characteristics of most of thermoplastics which agrees with other workers in this field. An alternative way to overcome this restriction consists in obtaining both components (matrix and filler) dispersed in water. In this way, high performance composite materials can be processed with a good level of dispersion by taking advantage of the hierarchical structure of cellulose and using a latex or a water soluble polymer to form the matrix [75, 76].

Cellulose microfibrils can be found as intertwined microfibrils in parenchyma cell wall. They can be

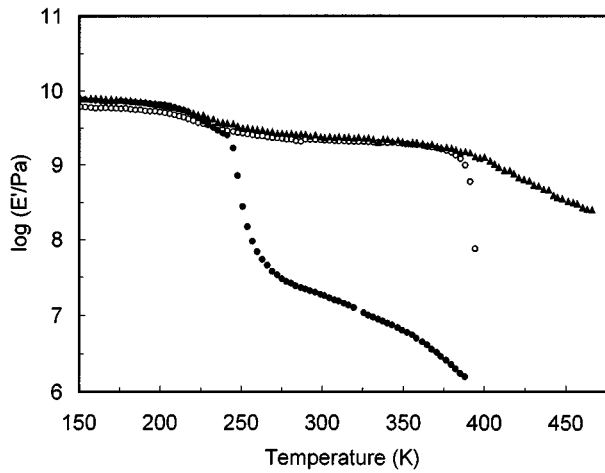


(a)

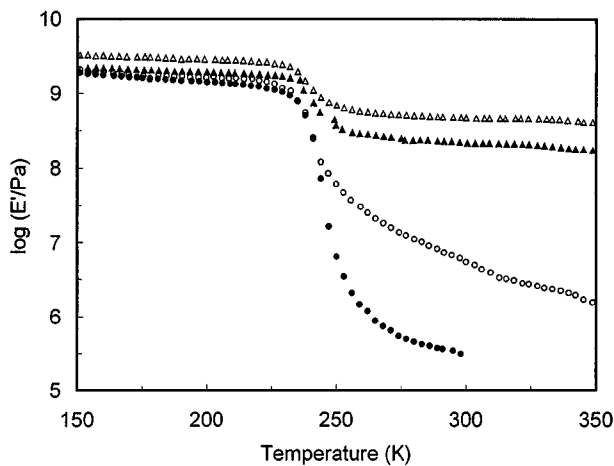


(b)

Figure 22 Transmission electron micrograph of a dilute suspension of (a) sugar beet cellulose microfibrils, and (b) tunicin.



(a)



(b)

Figure 23 Logarithm of the storage tensile modulus E' versus temperature at 1 Hz for (a) 30 wt% glycerol plasticised potato starch filled with 0 wt % (\bullet), 3.8 wt % (\circ), and 7.7 wt % (\blacktriangle) of potato pulp cellulose microfibrils, and (b) amorphous PHO films filled with 0 (\bullet), 1 (\circ), 3 (\blacktriangle) and 6 wt % (Δ) of tunicin whiskers.

extracted from the biomass by a chemical treatment leading to purified cellulose, followed by a mechanical treatment in order to obtain a homogeneous suspension due to the individualisation of the microfibrils. The microfibrils consist of monocrystalline cellulose domains with the microfibril axis parallel to the cellulose chains. As they are devoid of chain folding and contain only a small number of defects, each microfibril can be considered as a string of polymer whiskers, linked along the microfibril by amorphous domains, and having a modulus close to that of the perfect crystal of native cellulose (estimated to be 250 GPa). The amorphous regions act as structural defects and are responsible for the transverse cleavage of the microfibrils into short monocrystals, or whiskers, under acid hydrolysis.

Cellulose microfibrils and cellulose whiskers suspensions were obtained from sugar beet [78] or potato pulp [79], and from tunicin—a sea animal cellulose—[80–82] or wheat straw [83, 84]. Typical electron micrographs obtained from dilute suspensions of sugar beet cellulose microfibrils and tunicin whiskers are shown in Fig. 22. Individual microfibrils are almost 5 nm in width and the length is much higher, leading to a practically infinite aspect ratio of this filler. Tunicin whiskers consist of slender parallelepiped rods with lengths ranging from 100 nm to several μm (average value around 1 μm) and widths on the order of 10–20 nm. The aspect ratio was estimated from transmission electron microscopy and was around 70. Both kinds of filler can be used as a reinforcing phase in a polymer matrix. High performance nanocomposite materials are obtained by casting films from a mixture of polymer dispersion and cellulose suspension.

For instance, Fig. 23 shows the plot of the storage tensile modulus versus temperature for 30 wt% glycerol plasticised potato starch films reinforced by potato cellulose microfibrils (Fig. 23a) and poly(hydroxyoctanoate) (PHO) films reinforced by

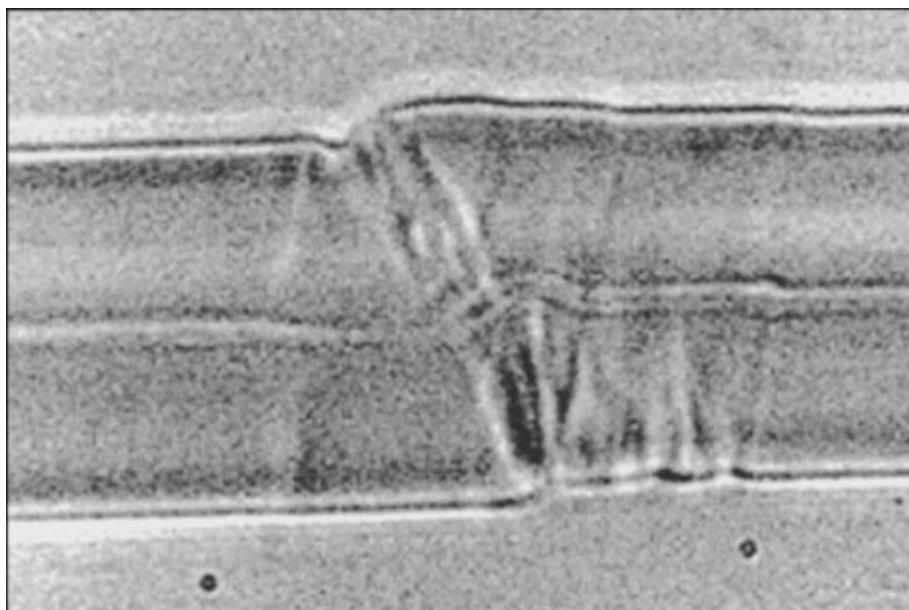


Figure 24 Micro-compressive defect (kink band) in a hemp fibre ultimate (unpolarised white light $\times 1000$ magnification).

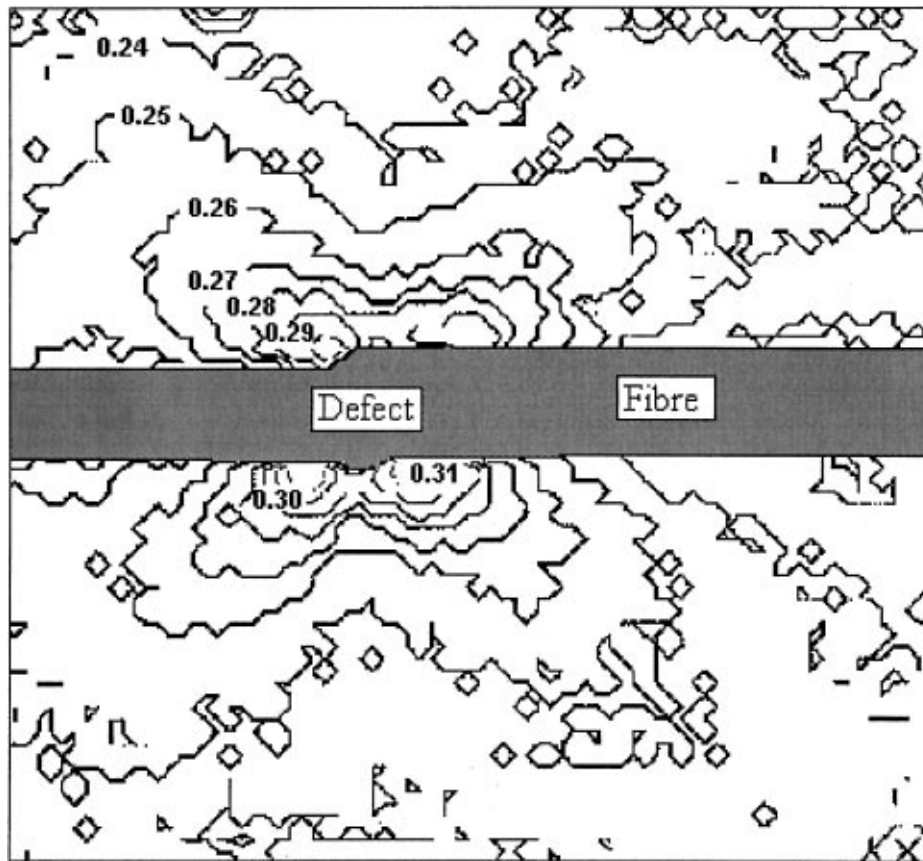


Figure 25 Contour map depicting the partial fringe order distribution in an epoxy matrix surrounding a single micro-compressive defect.

tunicin whiskers (Fig. 23b). Even at low filler content, these films display improved mechanical properties, especially at temperature higher than T_g of the matrix. Moreover, a stabilisation of the rubbery modulus is observed for 3 and 6 wt% PHO reinforced films up to 500 K (not shown), a temperature at which cellulose starts to decompose. Cellulose whiskers can be considered as model fillers and are suitable for calculations.

The high reinforcing effect of cellulose whiskers is ascribed to the presence of strong interactions between whiskers such as hydrogen bonds, which lead to the formation of a rigid network governed by the percolation threshold. For tunicin whiskers, the threshold fraction to reach percolation is close to 1% vol, which corresponds to ~ 1.5 wt%. This rigid whisker network which develops above the percolation threshold by hydrogen bonding allows a thermally stable plateau to be reached. The effect of factors such as the particle size of the latex [81] and the crystallinity of the matrix [82] on the percolation phenomenon were also investigated. A transcrystallization phenomenon of semi-crystalline PHO on cellulose whiskers was evidenced by dynamic mechanical analysis [82, 84].

8. Composite micromechanics

The measurement of the *in-situ stresses* and strains of fibres within composite materials has already been discussed (Eichhorn—UMIST, UK), but the role of defects in determining the local mechanics of composite materials is also a subject of great interest. Many methods have been applied to understanding this, one of which will be discussed in this section.

8.1. Bangor, Wales, UK—half fringe photoelasticity

One of the main problems in using natural fibres is the variability in mechanical properties of the fibres. Certain plant fibres, notably flax (*Linum usitatissimum*) and hemp (*Cannabis sativa*) possess tensile properties which make them potentially attractive for use as reinforcement in polymer matrix composites (PMC) [1, 2, 89]. These fibres are, however, susceptible to damage in compression through the formation of kink bands [90]. In flax, these micro-compressive (MC) defects, which are similar to the kinks formed in synthetic polymeric fibres [91], have been shown to reduce both the tensile modulus and ultimate strength of the fibre [92].

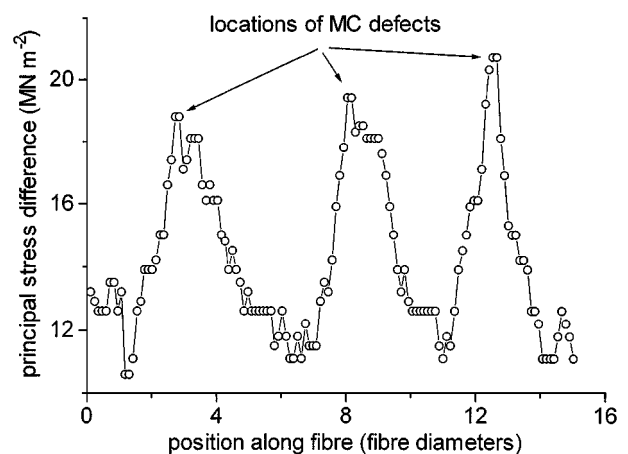


Figure 26 Distribution of the matrix principal stress difference parallel to the fibre-matrix interface and in close proximity to it.

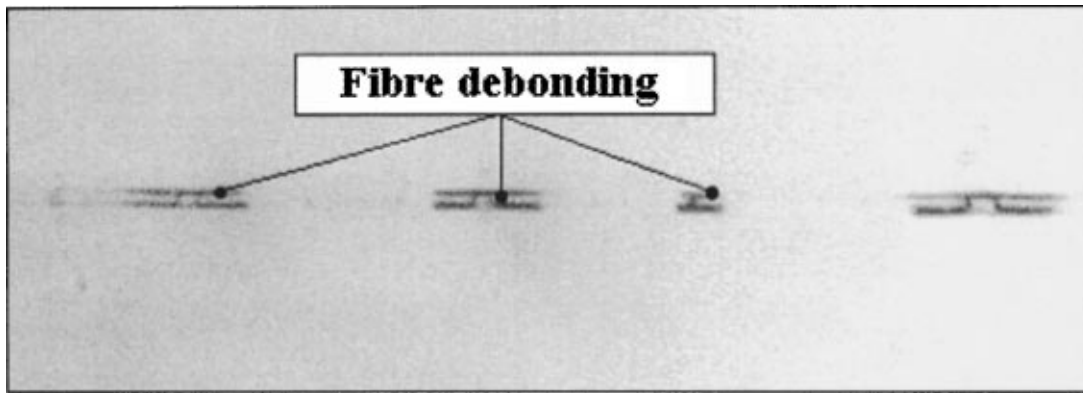


Figure 27 Debonded zones adjacent to fibre breaks in a failed SFC tensile specimen (unpolarised light $\times 100$ magnification).

In addition, it has been noted that these features act as loci of fibre failure [93]. In wood pulp fibres, MC (and other) defects have been noted to result in strain concentrations [94]. When strained in uniaxial tension parallel to the fibre axis, kink bands formed in high modulus polyethylene fibres have been shown to lead to stress concentrations in the surrounding (epoxy) matrix, which it was thought could stimulate fibre-matrix debonding [95]. In the work reviewed herein by Mark Hughes and Callum Hill, University of Wales it is considered that, similarly, in MC damaged hemp fibre, stress concentrations might well arise in the matrix surrounding the defects. These, it is believed, might have serious implications as far as composite behaviour is concerned. Half fringe photoelasticity (HFP) has been used to investigate this hypothesis and to quantify the magnitude of any stress concentrations [96, 97].

Developed in the early 1980s, HFP is a system which combines classical photoelasticity with modern digital image analysis, using computers [98, 99]. In this work, HFP was employed to analyse the stress field in an epoxy matrix, adjacent to MC defects in strained miniature composite tensile specimens. Each specimen was reinforced with a single hemp fibre ultimate (individual cell). A full description of the system used for this work and the calibration procedure adopted, has been reported elsewhere [97].

It has been demonstrated that stress concentrations do indeed arise in the matrix in the vicinity of MC defects when the single filament composites (SFC) are strained parallel to the fibre axis [96, 97]. Fig. 24 shows the morphology of a typical MC feature in a hemp fibre ultimate. Fig. 25 is a contour map depicting the partial fringe order distribution (which is equivalent to the principal stress difference, since the two are linearly related [100] around such a defect when the SFC was strained to approximately 0.5%. It has been observed that matrix stress concentration factors exceeding 1.4 (up to 1.65 has been recorded) can arise in close proximity to the interface [97].

It is believed that these stress concentrations arise because of heterogeneous fibre straining characteristics resulting from fibre damage, possibly exacerbated by the distinct morphology of the MC features. A mismatch in properties between those of the heterogeneous fibre and the homogeneous matrix probably results in an uneven interfacial shear stress distribution. This sup-

position is supported by the observation that the matrix principal stress difference distribution parallel to the fibre surface (but in close proximity to it), is decidedly irregular (Fig. 26). As may be noted, the maximum values for principal stress difference are recorded in the matrix adjacent to the MC defects. Since the principal stress difference can be related to shear stress [100] it might be inferred that, adjacent to MC defects, high interfacial shear stresses prevail. It is believed that these probably account for the debonded zones observed in failed SFCs (Fig. 27) [96, 97]. Furthermore, it has been noted that MC defects can occur at frequent intervals along the length of the fibre [97]. This may well have implications in terms of stress transfer between phases, critical fibre length and ultimately the reinforcing efficiency of micro-compressed fibres. Additionally, it is believed that stress concentrations can lead to the initiation of cracking in the matrix [96, 97]. As a result of these observations, it has been postulated that MC defects play a role in the deformation and fracture processes of bast fibre reinforced thermosetting PMCs and might affect, in particular, the toughness of these materials [96, 101].

9. Discussion and conclusions

The exploitation of natural fibres in industrial applications provides challenges for the research community to come up with effective ways of both analysing the modes of deformation of such materials, and in effecting the adhesion between matrix and fibre. In conjunction with this there is a need to more fully understand the basic structural components of the fibres, and their effect on the mechanical ensemble. It would appear that a wide variety of work is being conducted worldwide with some crossover of ideas and focus. The interface is one such area that has attracted a lot of interest, and new and cost effective ways of treating cellulose fibres, with the desirable end-properties, can only benefit exploitation. In the future, combination of modern testing techniques, such as Raman and miniature tensile testing, and the modification of fibre surfaces will lead to a better knowledge of desirable properties. Defect free fibres may not be possible, however the incorporation of purer crystalline cellulose, such as bacterial or animal sources, may be a way forward. However, the development of better processing for releasing the fibres

could be another focus for the research community. On a fundamental level the measurement and understanding of the role of defects in natural cellulose fibres may also see further development. Finally, to properly understand and measure the role of defects and the interface it is thought that a combination of techniques may be the only way to fully achieve this goal.

References

1. D. ROBSON, J. HAGUE, G. NEWMAN, G. JERONOMIDIS and M. ANSELL, in "Survey of Natural Materials for Use in Structural Composites as Reinforcement and Matrices" (Woodland Publishing Ltd, Abingdon, 1996).
2. J. BOLTON, *Outlook on Agriculture* **24** (1995) 85.
3. A. K. BLEDZKI and J. GASSAN, *Prog. Polym. Sci.* **24** (1999) 221.
4. E. T. N. BISANDA and M. P. ANSELL, *J. Mater. Sci.* **27** (1992) 1690.
5. A. N. SHAN and S. C. LAKKARD, *Fibre Sci. Technol.* **15** (1981) 41.
6. M. K. SRIDHAR and G. BASAVARAJAPPA, *Text. Res. J.* **7**(9) (1982) 87.
7. S. H. ZERONIAN, *J. Appl. Polym. Sci.* **47** (1991) 445.
8. P. J. ROE and M. P. ANSELL, *J. Mater. Sci.* **20** (1985) 4015.
9. A. J. MICHELL and D. WILLIS, *Appita* **31**(3) (1978) 347.
10. H. SAECHTLING, in "International Plastics Handbook" (Hanser, Munchen, 1987).
11. A. PAYEN, *C. R. Hebd. Seances Acad. Sci.* **7** (1838) 1052.
12. C. WOODCOCK and A. SARKO, *Macromolecules.* **13** (1980) 1183.
13. A. SARKO and R. MUGGLI, *ibid.* **7** (1974) 480.
14. W. G. GLASSER, in "Pulp and Paper Chemistry and Chemical Technology" (Wiley InterScience, New York, 1980) p. 39.
15. G. BUSCHLE-DILLER, C. FANTER and F. LOTH, *Text. Res. J.* **69** (1999) 244.
16. R. L. WHISTLER and E. L. RICHARDS, in "The Carbohydrates, 2A" (Academic Press, New York, 1970) p. 447.
17. A. J. PANSHIN and C. DE ZEEUW, "Textbook of Wood Technology" (McGraw-Hill, New York, 1970).
18. I. D. CAVE, *Forest Products Journal* **16** (1966) 37.
19. K. M. ENTWISTLE and N. J. TERRILL, *J. Mater. Sci.* **35** (2000) 1675.
20. V. K. MITRA, W. M. JR. RISEN and R. H. BAUGHMAN, *J. Chem. Phys.* **66** (1977) 2731.
21. D. N. BATCHELDER and D. BLOOR, *J. Polym. Sci. Polym. Phys. Edn.* **17** (1979) 569.
22. R. J. YOUNG, *J. Text. Inst.* **86** (1995) 360.
23. W. Y. HAMAD and S. J. EICHHORN, *ASME J. Eng. Mat. & Tech.* **119** (1997) 309.
24. S. J. EICHHORN, R. J. YOUNG and W.-Y. YEH, *Text. Res. J.* **71** (2001) 121.
25. S. J. EICHHORN, M. L. HUGHES, R. SNELL and L. MOTT, *J. Mater. Sci. Lett.* **19**(8) (2000) 721.
26. R. H. ATALLA and S. C. NAGEL, *Science* **185** (1974) 522.
27. M. G. NORTHOLT, *Polymer* **21** (1980) 1199.
28. I. M. WARD, "Mechanical Properties of Solid Polymers" (Wiley Inter Science, 1971) p. 253.
29. D. H. PAGE, F. EL-HOSSEINY, K. WINKLER and R. BAIN, *Pulp and Paper Magazine of Canada* **73**(8) (1972) 72.
30. F. EL-HOSSEINY and D. H. PAGE, *Fibre Science and Technology* **8** (1975) 21.
31. C. Y. KIM, D. H. PAGE, F. EL-HOSSEINY and A. P. S. LANCASTER, *Appl. Polym. Sci.* **19** (1975) 1549.
32. D. H. PAGE and F. EL-HOSSEINY, *Svenk Papperstidning* **14** (1976) 471.
33. D. H. PAGE, F. EL-HOSSEINY, K. WINKLER and A. P. S. LANCASTER, *TAPPI* **60** (1977) 114.
34. D. H. PAGE and F. EL-HOSSEINY, *Journal of Pulp and Paper Science* **84** (1983) 99.
35. O. J. KALLMES and M. PEREZ, *Proceedings of the Technical Sec. British Paper Board Makers Association* **1** (1966) 507.
36. C. A. JENTZEN, *TAPPI* **47** (1964) 412.
37. J. NYREN, *Pulp and Paper Magazine of Canada* **72** (1971) 81.
38. N. HARTLER and J. NYREN, *TAPPI—Special Technical Association Publication* **8** (1970) 265.
39. P. M. WILD, J. W. PROVAN, S. POP and R. GUIN, *TAPPI J.* **4** (1999) 209.
40. P. C. KERSAVAGE, Bulletin 790, USDA, 1973.
41. L. MOTT, S. M. SHALER, L. H. GROOM and B. LIANG, *TAPPI* **78** (1995) 143.
42. B. A. JAYNE, *TAPPI J.* **6** (1959) 461.
43. D. C. MCINTOSH, *ibid.* **46** (1963) 237.
44. L. H. GROOM, S. M. SHALER and L. MOTT, in Proceedings of the 1995 International Paper Physics Conference, Niagara-on-the-Lake, Ontario, September 1995 (Canadian Pulp and Paper Association, Montreal, 1995) p. 13.
45. L. MOTT, Ph.D. Thesis, Univ. of Maine, Orono, Maine, 1995, p. 198.
46. L. H. GROOM, S. M. SHALER and L. MOTT, in Proceedings of the Forest Products Society Southeast Section Annual Meeting, Atlanta, November 1994 (Forest Products Society, Madison) p. 20.
47. L. MOTT, S. M. SHALER, L. H. GROOM and B. H. LIANG, *TAPPI J.* **5** (1995) 143.
48. S. M. SHALER, L. H. GROOM and L. MOTT, in Proceedings of the Woodfiber/Plastic Composites: Virgin and Recycled Wood Fibre and Polymers for Composites, 7293, Madison, May 1995 (Forest Products Society, Madison, 1996) p. 25.
49. S. M. SHALER, L. MOTT and L. H. GROOM, in Post-conference Proceedings of the 1996 VIII International Congress on Experimental Mechanics, Nashville, June 1996 (Society for Experimental Mechanics, Bethel, CT, 1996) p. 196.
50. L. H. GROOM, S. M. SHALER and L. MOTT, in Proceedings of the Woodfiber/Plastic Composites: Virgin and Recycled Wood Fibre and Polymers for Composites, Proceedings No. 7293, Madison, May 1995 (Forest Products Society, Madison, 1996) p. 33.
51. R. SNELL, J. HAGUE and L. H. GROOM, in Proceedings of the Fourth International Conference on Woodfiber-Plastic Composites, Madison, May 1997 (Forest Products Society, Madison, 1997) p. 5.
52. L. H. GROOM, L. MOTT and S. M. SHALER, in Proceedings of the International Workshop on the Significance of Microfibril Angle to Wood Quality, Westport, NZ, October 1997, edited by B. Butterfield, p. 375.
53. L. H. GROOM and T. PESACRETA, in Proceedings of the Fourth International Conference on Woodfiber-Plastic Composites, Madison, May 1997 (Forest Products Society, Madison, 1997) p. 26.
54. L. H. GROOM, S. M. SHALER and L. MOTT, in Proceedings of the First European Panel Products Symposium, Llandudno, Wales, October 1997, edited by J. Hague, C. Loxton, J. Bolton and L. Mott, p. 53.
55. L. H. GROOM, L. MOTT and S. M. SHALER, in Proceedings of the 33rd Annual International Particle board/Composite Materials Symposium, Pullman, WA, April 1999, edited by M. Wolcott, R. Tichy, D. Bender and L. Miklosko (Washington State University, Pullman, WA) p. 89.
56. P. MOSS and L. H. GROOM, in "Handbook of Physical Testing of Paper," Vol. 2, 2nd ed. (Marcel Dekker, Inc., New York, in press).
57. R. SNELL, L. H. GROOM and T. G. RIALS, *Holzforschung*, in press.
58. G. CANCHÉ-ESCAMILLA, J. I. CAUICH-CUPUL, E. MENDIZABAL, J. E. PUIG, H. VÁZQUEZ-TORRES and P. J. HERRERA-FRANCO, *Composites: Part A* **30** (1999) 349.
59. G. CANCHÉ-ESCAMILLA, G. RODRÍGUEZ TRUJILLO, P. J. HERRERA-FRANCO, E. MENDIZABAL and J. E. PUIG, *J. Appl. Polym. Sci.* **66** (1997) 339.
60. N. M. WHITE and M. P. ANSELL, *J. Mater. Sci.* **18** (1983) 1549.
61. R. A. CLARK and M. P. ANSELL, *ibid.* **21** (1986) 269.
62. E. T. N. BISANDA and M. P. ANSELL, in "Cellulose Sources and Exploitation" (Ellis Horwood, 1990) p. 235.
63. *Idem.*, *Composite Science and Technology* **41** (1991) 165.
64. L. Y. MWAIKAMBO and E. T. N. BISANDA, *Polymer*

- Testing* **18** (1999) 181.
65. L. Y. MWAIKAMBO, E. MARTUSCELLI and M. AVELLA, *ibid.* in press.
 66. L. Y. MWAIKAMBO and M. P. ANSELL, *Die Angewandte Makromolekulare Chemie* **272** (1999) 108.
 67. G. G. DIJON, M.Phil. to Ph.D. Transfer Report, Department of Materials, Imperial College of Science and Technology and Medicine, London, 1999.
 68. A. STAMBOULIS, C. BAILLIE, M. PIACESI and E. SCHULTZ, in Proceedings of the 12th International Conference on Composite Materials, Paris, July 1999.
 69. A. STAMBOULIS, C. BAILLIE and E. SCHULTZ, in Proceedings of the 2nd International Wood and Natural Fibre Composites Symposium, Kassel, Germany, June 1999, p. 101.
 70. N. E. ZAFEIROPOULOS, A. H. BARBER, C. A. BAILLIE and F. L. MATTHEWS, in Proceedings of the 5th International Conference on Deformation and Fracture of Composites, London, March 1999 (IOM Communications) p. 282.
 71. N. E. ZAFEIROPOULOS, C. A. BAILLIE and F. L. MATTHEWS, *Composites Part A*, accepted for publication.
 72. H. D. WAGNER, A. LUSTIGER, C. N. MARZINSKY and R. R. MUELLER, *Comp. Sci. Tech.* **48** (1992) 181.
 73. R. M. ROWELL, A.-M. TILLMAN and R. SIMONSON, *J. Wood. Chem. Tech.* **6** (1986) 427.
 74. N. E. ZAFEIROPOULOS, C. A. BAILLIE and F. L. MATTHEWS, in Proceedings of the 9th European Conference on Composite Materials, Brighton, June 2000.
 75. A. DUFRESNE, *Recent Research Developments in Macromolecular Research* **3** (1998) 455.
 76. A. DUFRESNE and J. Y. CAVAILLE, in "Biopolymers : Utilizing Nature's Advanced Materials" edited by S. H. Imam, R. V. Greene and B. R. Zaidi (ACS Symposium Series 723, 1999) p. 39.
 77. A. DUFRESNE, J. Y. CAVAILLE and M. R. VIGNON, *J. Appl. Polym. Sci.* **64** (1997) 1185.
 78. A. DUFRESNE and M. R. VIGNON, *Macromolecules* **31** (1998) 2693.
 79. V. FAVIER, G. R. CANOVA, J. Y. CAVAILLE, H. CHANZY, A. DUFRESNE and C. GAUTHIER, *Polym. Adv. Tech.* **6** (1995) 351.
 80. D. DUBIEF, E. SAMAIN and A. DUFRESNE, *Macromolecules* **32** (1999) 5765.
 81. A. DUFRESNE, M. B. KELLERHALS and B. WITHOLT, *ibid.* **32** (1999) 7396.
 82. W. HELBERT, J. Y. CAVAILLE and A. DUFRESNE, *Polym. Compos.* **17** (1996) 604.
 83. A. DUFRESNE, J. Y. CAVAILLE and W. HELBERT, *ibid.* **18** (1997) 198.
 84. A. DUFRESNE, *Compos. Interfaces* **7** (2000) 53.
 85. J. M. FELIX and P. GATENHOLM, *J. Mater. Sci.* **29** (1994) 3043.
 86. F. P. LIU, T. G. RIALS, M. P. WOLCOTT and D. J. GARDNER, in Proceedings of the 2nd Woodfibre-Plastic Composites Conference, May 1-3, 1995 (Forest Products Society, Madison, WI) p. 74.
 87. F.-P. LIU, M. P. WOLCOTT, D. J. GARDNER and T. G. RIALS, *Composite Interfaces* **2** (1994) 419.
 88. T. G. RIALS and J. SIMONSEN, *ibid.* in press.
 89. J. BOLTON, *Mat. Tech.* **9** (1994) 12.
 90. H. L. BOS and A. M. DONALD, *J. Mater. Sci.* **34** (1999) 3029.
 91. D. C. MARTIN and E. L. THOMAS, *J. Mat. Sci.* **26** (1991) 5171.
 92. G. C. DAVIES and D. M. BRUCE, *Tex. Res. J.* **68** (1998) 623.
 93. B. FOCHER, A. MARZETTI and H. S. S. SHARMA, in "The Biology and Processing of Flax" (M Publications, Belfast, 1992) p. 333.
 94. L. MOTT, S. M. SHALER and L. H. GROOM, *Wood and Fibre Science* **28** (1996) 429.
 95. D. T. GRUBB and Z.-F. LI, *J. Mater. Sci.* **29** (1994) 203.
 96. M. HUGHES, L. MOTT, J. HAGUE and C. A. S. HILL, in Proceedings of the 5th International Woodfiber-Plastics Conference, Madison, WI, May 26-29, 1999 (Forest Products Society, Madison, WI, 1999) p. 175.
 97. M. HUGHES, C. HILL, G. SÈBE, J. HAGUE, M. SPEAR and L. MOTT, *Composite Interfaces* **7** (2000) 13.
 98. A. S. VOLOSHIN and C. P. BURGER, *Experimental Mechanics* **23** (1983) 304.
 99. C. P. BURGER, in "Handbook on Experimental Mechanics," edited by A. S. Kobayashi (Society for Experimental Mechanics, Bethel, USA, 1993) p. 248.
 100. J. W. DALLY and W. F. RILEY, in "Experimental Stress Analysis" (McGraw-Hill Book Company, New York, 1965) p. 143.
 101. G. SÈBE, N. S. CETIN, C. A. S. HILL and M. HUGHES, *Applied Composite Materials* **7** (2000) 341.

*Received 5 October
and accepted 24 October 2000*